

https://dspace.org/

The expression and purification of the fab fragment of ibalizumab: a monoclonal anti-CD4 antibody with potent HIV inhibitory effects

Munshi, Rafeeqah

2016
http://hdl.handle.net/10539/22458

Downloaded from a DSpace repository. https://dspace.org/

The expression and purification of the Fab fragment of Ibalizumab: a monoclonal anti-CD4 antibody with potent HIV inhibitory effects



Rafeeqah Munshi

A dissertation submitted to the Faculty of Health Sciences, University of the Witwatersrand, in fulfillment of the requirements for the degree of Master of Science in Medicine

Johannesburg 2016

Declaration

I, Rafeeqah Munshi, declare that this dissertation is my own work. It is being submitted for the degree of Masters of Science in Medicine in the University of the Witwatersrand, Johannesburg. It has not been submitted before for any degree or examination at this or any other University.

…… **……**

Signature **Date**

PLAGIARISM DECLARATION TO BE SIGNED BY ALL HIGHER DEGREE STUDENTS

SENATE PLAGIARISM POLICY

I **Rafeeqah Munshi** (Student number: **353 141**) am a student registered for the degree of **MSc (Med)** in the academic year **2016**.

I hereby declare the following:

- I am aware that plagiarism (the use of someone else's work without their permission and/or without acknowledging the original source) is wrong.

- I confirm that the work submitted for assessment for the above degree is my own unaided work except where I have explicitly indicated otherwise.

- I have followed the required conventions in referencing the thoughts and ideas of others.

- I understand that the University of the Witwatersrand may take disciplinary action against me if there is a belief that this is not my own unaided work or that I have failed to acknowledge the source of the ideas or words in my writing.

Signature: _____ Date: _____

Dedication

To my parents Abubukr and Naziema who bring purpose to my life. You are my home, my beacon, my strength.

To my siblings Imraan, Naadhirah and Saadia for motivating me to be the best I can be.

And to My aunt Faatima, who would have been so proud.

Abstract

Infection with Human Immunodeficiency Virus (HIV), the causative agent of Acquired Immunodeficiency Syndrome (AIDS), remains one of the most significant healthcare challenges facing South Africa. The development of alternative therapeutic strategies targeting different stages of the viral life cycle remains an important ongoing biomedical research objective. Recently, a monoclonal antibody which binds CD4, the primary cellular host receptor of HIV, has shown outstanding antiviral efficacy in Phase II clinical trials. However, the high costs associated with conventional therapeutic monoclonal antibody production, which involves expression, assembly and secretion of full-length antibodies using large-volume mammalian cell cultures; limit the clinical use of such compounds in the South African public healthcare setting. Accordingly, this study investigated the feasibility of generating a functional Ibalizumab Fab ($IBLZ_{Fab}$) fragment using an *E. coli*-based expression system. Heavy and Light Variable (VH/VL) Ibalizumab chains were expressed in BL21 *E. coli* and functional Fab fragments were reconstituted by oxidative refolding in the bacterial periplasm. The success of reconstitution and efficacy of the Fab fragment was assessed *in vitro* by analytical SDS-PAGE, Surface Plasmon Resonance (SPR) and cell culture models of HIV infection. The calculated CD4-binding affinity (K_{DJ} of $IBLZ_{Fab}$ was 11.3 nM, which compares favorably with the (K_D) values of most antibody-antigen interactions, which are typically in the low nanomolar (nM) range. Viral inhibition studies were also performed to evaluate whether the Fab fragment had any detectable neutralization activity. Even though neutralization activity was obtained at a high concentration the bacterially expressed $IBLZ_{Fab}$ fragment was able to inhibit CAP210 viral entry, illustrating the feasibility of expressing and purifying functional Ibalizimab Fab fragments using a bacterial expression system. Ongoing efforts are focused on improving yields of purified $IBLZ_{Fab}$ through optimization of the expression and purification methods employed.

Acknowledgements

I would like to acknowledge and extend my heartfelt gratitude to the following individuals and institutions:

My supervisor Dr. Nichole M. Cerutti for the continuous support and encouragement. For keeping me sane when I faltered and for guiding me throughout this journey. Your frequent jokes and friendly smile always comforted me in the dimmest of times. I sincerely thank you for having the patience and understanding you've extended to me both inside the laboratory and beyond.

My co-supervisor Dr. Alexio Capovilla for granting me the opportunity to work on this project. For allowing me to overcome the fear of the unknown and for igniting the scientific curiosity within me. Without your inspiring words and guidance, I would not stand where I am today. I am truly grateful for all that you have taught me.

Dr Mark Killick for showing me the ropes and assisting me with the neutralization studies. Thank you for your patience and understanding. You are an exceptional teacher.

The head of the HIV Pathogenesis Research Unit (HPRU), Prof. Maria Papathanasopoulos, for welcoming me into the HPRU family with open arms. Your infectious personality and warm smile made each day enjoyable.

My parents, Naziema and Abubukr for your endless love and support and for putting up with my moods during the tougher days. You are truly my strength.

My cherished friends and colleagues who I have been so privileged to have come across. You made each day exciting. Mr Dean Harris for all the laughs and assistance, you are a one of the kindest people I know; Mr Roberto Pereira who shared this journey with me, your life lessons and ideals are truly refreshing – Google's got nothing on you; Dr Irene Ketsoglou for all your support and kind-heartedness; Ms Nancy Tumba, Mrs Michelle Grant and Dr Gavin Owen for making this voyage that much better.

This study was generously supported by the Poliomyelitis Research Fund, the South African Medical Research Council, the National Research Foundation and the Belgian Technical Cooperation.

Table of Contents

1 Chapter 1: Introduction 1-1

1.1 HIV life cycle 1-1

1.2 HIV entry into host CD4-positive cells 1-2

1.3 Current HIV treatment regimens 4

1.4 Monoclonal Antibody (mAb) therapy 6

1.4.1 mAb derivatives 9

1.4.2 Monoclonal antibodies used in biopharmaceutical applications and therapies 10

1.5 The anti-CD4 monoclonal antibody: Ibalizumab 15

1.6 Aim and Objectives 21

2 Chapter 2: Experimental procedures 22

2.1 Cloning of $IBLZ_{Fab}$ expression cassettes 22

2.1.1 Preparation of $IBLZ_{Fab}$-Encoding DNA for subcloning (Digestion and ligation of pET15b plasmid vector and $IBLZ_{Fab}$ Fragment) 23

2.2 Expression of the $IBLZ_{Fab}$ fragment in Bacterial Cell Culture 25

2.3 Extraction and Purification of $IBLZ_{Fab}$ 25

2.3.1 Extraction of protein expression 25

2.3.2 Purification procedure of $IBLZ_{Fab}$ 26

2.4 Expression and Purification of 2 domain CD4 (2dCD4) 28

2.4.1 Purification of 2dCD4 28

2.5 Functionality testing of $IBLZ_{Fab}$ 30

2.5.1 Enzyme-linked Immunosorbent Assay (ELISA) 30

2.5.2 Surface Plasmon Resonance (SPR): Analysis of the 2dCD4-$IBLZ_{Fab}$ interaction 32

2.5.3 Viral inhibition: Neutralization assays of $IBLZ_{Fab}$ 32

3 Chapter 3: Results 35

3.1 Generation of recombinant Bicistronic $IBLZ_{Fab}$-expression vectors 35

3.2 Expression and purification of $IBLZ_{Fab}$ 35

3.2.1 Size exclusion chromatography 40

3.3 Functionality testing of $IBLZ_{Fab}$ 42

3.3.1 Enzyme-linked Immunosorbent Assay (ELISA) Analysis of $IBLZ_{Fab}$ 42

3.3.2 Surface Plasmon Resonance (SPR) Analysis of $IBLZ_{Fab}$ 46

3.3.3 Viral inhibition: Neutralization Assays of $IBLZ_{Fab}$ 48

4 Chapter 4: Discussion and Concluding remarks 51
4.1 Concluding Remarks 57
5 References 60
6 Ethics i
Appendix 1: Customary Protocols and Recipes ii
Solutions for bacterial culture ii
Luria-Bertani (LB) Broth (1L) ii
Agar plates ii
Ampicillin stock (100 mg/ml) ii
Transformation buffer (100mls) (for chemically competent cells) ii
Preparation of competent bacterial cell (DH5α and BL21 (DE3) stars ii
Transformation of competent E. coli cells iii
Solutions for Agarose Electrophoresis iii
Preparation of agarose gels iii
Electrophoresis Procedure iii
Protein purification iv
Solutions for protein Purification of 2dCD4 iv
Preparation of columns for purification procedures v
Solutions for Denaturing Discontinuous Electrophoresis v
Preparation of SDS-PAGE gels vi
Casting of SDS-PAGE gels vi
Electrophoresis procedure vi
Staining procedures vii
Protocol for de-staining procedures vii
Western Blotting solutions and procedure vii
Western blotting Procedures viii
BCA Assay (Thermo Fisher Scientific; Massachusetts, USA) viii
Appendix 2: Nucleotide sequence of recombinant Ibalizumab Fab Fragment and pET15b Expression vector ix
Nucleotide sequence of recombinant Ibalizumab Fab Fragment ix
pET15b Expression vector of the recombinant Ibalizumab Fab fragment xii
Sequence similarity of Ibalizumab Fab fragment construct xiii

Appendix 3: Supplementary Figures xiv

List of figures

Figure 1. Outline of HIV entry: 3
Figure 2. Structural schematic of an antibody: 8
Figure 3.Broadly neutralizing antibodies that target the HIV Env spikes: 14
Figure 4. Three-dimensional structure of a complex of 2dCD4, the Fab fragment of Ibalizumab, gp120 and the Fab fragment of 17b (obtained through structural alignment of the Ibalizumab Fab fragment and gp120 associated with 2dCD4) 17
Figure 5. Schematic representation of the bacterial IBLZ Fab ($IBLZ_{fab}$) expression cassette: 23
Figure 6. Restriction digestion analysis of the pET15b $IBLZ_{Fab}$ expression vector: 37
Figure 7. Western blot analysis of $IBLZ_{Fab}$ expression and purification under non-reducing conditions: 39
Figure 8. Elution profile of SEC separation on a Sephadex G-75 column, SDS-PAGE and western blot analysis of $IBLZ_{Fab}$ 41
Figure 9. Detection of $IBLZ_{Fab}$ bound 2dCD4: 43
Figure 10. Detection of the interaction between WT 2dCD4 and gp120-BAL in the presence of $IBLZ_{Fab}$: 45
Figure 11. 2dCD4-$IBLZ_{Fab}$ interaction analysis by SPR: 47
Figure 12. Non-reducing SDS-PAGE Analysis of 3 µg of total fraction of $IBLZ_{Fab}$: 49
Figure 13. Neutralization Assay of pseudoviruses CAP210, SF162 and VSV-G against entry inhibitor Enfuvirtide (T_{20}) and $IBLZ_{Fab}$: 50

List of Table(s)

Table 1. Summary of reduction in viral loads as observed in Ibalizumab clinical trials 18

List of Abbreviations

Abbreviations used in this thesis describe the following unless otherwise indicated:

ɣ Gamma

2dCD4 two-domain CD4

6HBsix-helix bundle

ADCC Antibody-Dependent Cellular Cytotoxicity

AIDS Acquired Immune Deficiency Syndrome

ARV antiretroviral

ART antiretroviral therapy

bNAbs broadly Neutralizing Antibodies

biNAb bispecific bNAb

bp base pairs

BSA Bovine Serum Albumin

C constant region

CA p24 capsid protein

CCR5 Chemokine (C-C Motif) Receptor 5

CD4 Cluster of Differentiation 4

CD4+ CD4 Positive

CD4bs CD4-binding site

CD4i CD4-induced

CDC Centers for Disease Control

CDC Complement-Dependent Cytotoxicity

CDRL Complementarity-Determining Region of the Light chain

CHO Chinese Hamster Ovary

CroFab Crotiladae Polyvalent Immune Fab

CXCR4 Chemokine (C-X-C motif) Receptor 4

D Domain

dH_2O distilled water

DigiFab Digoxin immune Fab

DMEM Dulbecco's Modified Eagles Medium

DNA Deoxyribonucleic Acid

DTT dithiothreitol

E. coli *Escherichia coli*

EDTA Ethylenediamine Tetra Acetic Acid

EI Entry Inhibitor

ELISA Enzyme Linked Immunosorbant Assay

Env envelope glycoprotein

ESCRT Endosomal Sorting Complex Required for Transport

Fab antigen binding fragment of an antibody

Fc Fragment crystallizable

FCS Fetal Calf Serum

gp120 glycoprotein 120

gp120BaL subtype B envelope glycoprotein 120

gp41 glycoprotein 41

GSH reduced glutathione

GSSG oxidized glutathione

HAART Highly Active Antiretroviral Therapy

HIV Human Immunodeficiency Virus

HR Helical Region

HR1 Heptad Repeat helix 1

HR2 Heptad Repeat helix 2

HRP Horseradish Peroxidase

IBLZ Ibalizumab

$IBLZ_{Fab}$ Ibalizumab Fab fragment

$IBLZ_{H}$ variable heavy chain of Ibalizumab

$IBLZ_{L}$ variable light chain of Ibalizumab

IC_{50} 50percent inhibition

Ig immunoglobulin

IMAC Immobilized Metal-Affinity Chromatography

IN integrase

IPTG Isopropyl β-D-1-Thiogalactopyranoside

K kappa

kDa kilodalton

L lambda

LB Luria-Bertani broth

LEDGF Lens Epithelium-Derived Growth Factor

LMW Low Molecular Weight

LTR Long Terminal Repeat

mAb monoclonal Antibody

MCS Multiple Cloning Site

MHC Major Histocompatibility Complex

MHCII Major Histocompatibility Complex class II

MPER Membrane Proximal External Region

mRNA messenger RNA

MW Molecular Weight

Nab Neutralizing Antibody

Nef Negative effector

NK Natural Killer

OmpA Outer-Membrane Protein A

PAGE Polyacrylamide Gel Electrophoresis

PBS Phosphate Buffered Saline

PBS-T Phosphate Buffered Saline containing Tween-20

PDB ID Protein Data Bank Identification number

PIC Pre-Integration Complex

Pol Polymerase

RAG Recombination Activating Gene

RBS Ribosomal Binding Site

RNA Ribonucleic Acid

RT Reverse Transcriptase

sCD4 soluble 4 domain CD4

scFv single-chain Fv fragment

SDS-PAGE Sodium Dodecyl Sulfate Polyacrylamide Gel Electrophoresis

SEC Size Exclusion Chromatography

SFMII Serum Free Media II

SPR Surface Plasmon Resonance

TBS Tris Buffered Saline

TCR T-cell Receptor

$TCID_{50}$ Median Tissue Culture Infectious Dosage

Tris *Tris*(hydroxymethyl)aminomethane

T-TBS Tween-Tris Buffered Saline

US-FDA United States Food and Drug Administration

UV ultraviolet

V variable region

VH variable heavy chain

WHO World Health Organization

WT Wild-Type

X4 virus CXCR4 co-receptor using virus

X4/X5 virus either CXCR4 or CCR5 using virus

X5 CCR5 co-receptor using virus

1 Chapter 1: Introduction

The Human Immunodeficiency Virus (HIV), the causative agent of Acquired immunodeficiency Syndrome (AIDS), remains one of the most significant public healthcare challenges facing South Africa, with approximately 6.4 million individuals infected (12.2 % prevalence) [1]. According to the World Health Organization there were approximately 36.9 million people living with HIV at the end of 2014 with 2 million newly infected patients [2]. Sub-Saharan Africa accounted for 70 % (25.8 million) of new infections globally. To date 34 million people have died from HIV-related causes globally and no effective vaccine or eradicative cure is currently available [1].

AIDS was first described as a disease in 1981 by the Centers for Disease Control (CDC) of the United States [3, 4]. The initial description of the high risk sexual behavior group included patients receiving blood transfusions, intravenous drug users and homosexual or bisexual males [3].

1.1 HIV life cycle

HIV is a slow replicating retrovirus, belonging to the *Retroviridae* family that arose from several zoonotic transmissions of the simian immunodeficiency viruses over the past century [5]. HIV-1 infects CD4 T-helper cells, macrophages and dendritic cells thereby disrupting both the adaptive and innate immune responses [6]. Viral replication occurs through a series of steps that are initiated when the envelope glycoprotein spikes on the virus effectively engage the host cell surface receptor, CD4 and the co-receptor CC-chemokine receptor 5 (CCR5) or chemokine (C-X-C motif) receptor 4 (CXCR4) [7]. This attachment allows fusion of the viral membrane to the host cellular membrane and entry of the virus particle into the cell. Once inside the cell, the viral capsid protein partially uncoats, allowing for reverse transcription of the viral RNA genome, and the viral RNA genome then allows formation of the pre-integration complex (PIC) [8].

The PIC complex is then imported into the nucleus where PIC-associated integrase supported by host chromatin-binding protein lens epithelium-derived growth factor (LEDGF) coordinates the formation of the integrated provirus [9]. Host RNA polymerase II mediates transcription of the integrated provirus, and the mRNA strands are then exported from the nucleus by host protein factors, where the structural proteins are produced [9]. Assembly of virus-like particles takes place at the plasma-membrane. Once complete, ESCRT (endosomal sorting complex required for transport) complexes mediate viral-particle budding and release from the cell [10]. The last step of the viral life-cycle is maturation which occurs subsequent to budding. Protease-mediated maturation through proteolysis of precursor proteins turns the nascent virus particles into infectious virions [11].

Each step in the viral life-cycle presents an opportunity for the development of new drug targets. Since binding and entry into the host cell play a fundamental role in viral tropism and infection efficiency [7], exploiting our understanding of HIV entry may likely provide targets for novel drug treatments.

1.2 HIV entry into host CD4-positive cells

HIV entry is a multistep process that involves the binding of virions to the target cell, primarily via surface expressed CD4 receptors [7] (Figure 1). CD4 receptor binding occurs through the gp120 protein of the viral envelope. The envelope protein is a heavily glycosylated trimer comprised of gp120 and gp41 heterodimers [12] .The initial association between gp120 and the host cell is non-specific electrostatic interactions between the positively charged domains on gp120 and negatively charged proteoglycans on the host cell surface [13].

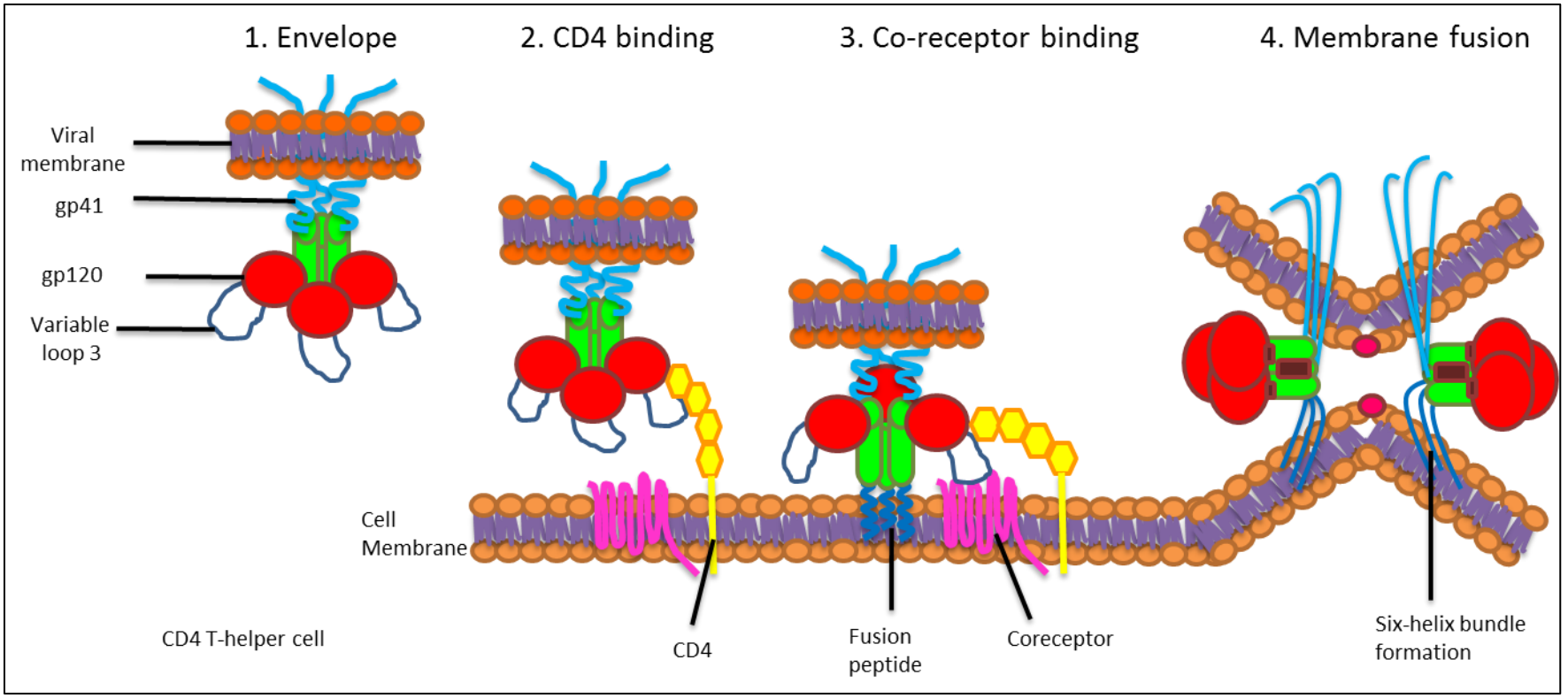

Figure 1. Outline of HIV entry:

To gain access to CD4 T-helper cells, macrophages and/or dendritic cells, the HIV envelope (Env), made up of gp120 and gp41 subunits (1), attaches to the cell surface receptor CD4 (2). The subsequent conformational change in Env allows co-receptor binding (3) and the beginning of the fusion process by the formation of the fusion peptide and the six-helix bundle (4). (Adapted from [7]).

Binding of viral gp120 to CD4 results in the rearrangement of the variable regions of gp120 (V1, V2 and V3) (Figure 1). This causes the formation of a bridging sheet which is made up of two double-stranded β sheets that are spatially separated in the unliganded state [14]. The conformational changes in gp120 allows the bridging sheet together with the extended V3 loop to interact with the co-receptor of choice, either CCR5 or CXCR4 [14]. CD4 projects further from the cell surface than chemokine receptors and therefore CD4 is required to bend after engagement with gp120 in order for the complex to be associated with the co-receptor [15]. Attachment of gp120 to the co-receptor is followed by fusion of the viral and host cell membranes [7]. This process involves the formation of a gp41 complex that results in a six-helix bundle (6HB, Figure 1) which leads to the development of a fusion pore and entry of viral contents into the cell [7]. The exposure of the hydrophobic gp41 fusion peptide is triggered by co-receptor binding [16]. The fusion peptide pierces the host cell membrane and allows heptad repeats from each gp41 subunit in the trimer to fold at the hinge region bringing an amino-terminal helical region (HR-N) and a carboxy-terminal helical region (HR-C) together; bringing the viral membrane and the host membrane into close proximity via the 6HB [7]. This rearrangement initiates the formation of the fusion pore and the eventual entrance of the viral capsid into the host cell [15, 16] (Figure 1).

Once inside the host cell, viral RNA is converted into double stranded DNA before being integrated into the host genome by viral reverse transcriptase and integrase, respectively. The viral DNA serves as a template for the transcription of novel RNA genomes, which are packaged into mature, infectious viruses that bud off at the cell surface [1].

1.3 Current HIV treatment regimens

There are four major drug classes for the treatment of HIV: entry inhibitors, reverse transcriptase inhibitors, integrase inhibitors and protease inhibitors. Highly active antiretroviral therapy (HAART) is the combination of two or more classes of drugs for the synergistic control of HIV

infection [14]. Existing antiretroviral therapy (ART) has dramatically reduced the morbidity and mortality associated with HIV/AIDS, but therapy is still associated with high costs, toxic side-effects and, most importantly, the emergence of drug-resistant viral strains. Thus, the development of alternative therapeutic strategies targeting different stages of the viral life cycle remains an important ongoing research objective.

Entry inhibitors have become increasingly popular candidate antiviral compounds due to their activity against multi-drug resistant viruses [17]. One advantage of targeting HIV entry is the extracellular site of action which is easily accessible and does not require intracellular transport of drug compounds such as RT or protease inhibitors. There are currently two entry inhibitors approved for the treatment of HIV-infected patients; the CCR5 antagonist Maraviroc and the fusion inhibitor Enfuvirtide [15].

Enfuvirtide, a fusion inhibitor, was the first entry inhibitor approved for treatment of HIV-1 infection in 2003 [15]. Enfuvirtide is a 36 amino acid long synthetic peptide based on the HR2 sequence of gp41. The HR2 region plays a crucial role in the formation of the 6HB during membrane fusion by interacting with HR1 [18]. This peptide disrupts the formation of the 6HB by competing with HR2 of gp41 for binding with HR1 [18, 19]. Maraviroc is a CCR5 antagonist, which is only effective against HIV strains that use CCR5 co-receptors during viral entry; as a consequence, it is recommended that patients undergo tropism testing before administering Maraviroc as part of the treatment regime [20]. There are, however, disadvantages to the use of entry inhibitors, such as the potential disruption of host receptor function (in the case of compounds that target host factors), while the sequence and structural diversity of the Env protein frequently leads to differences in potency of antiviral entry inhibitors against different viral strains [21]. Despite this, entry inhibitors are of special interest as they target a pivotal step in the life-cycle of the virus.

1.4 Monoclonal Antibody (mAb) therapy

Antibodies are host glycoproteins that make up one of the primary effectors of the adaptive immune response. They are produced by specialized B lymphocytes, known as plasma cells, in response to the presence of non-self or foreign molecules. Antibodies can directly inactivate antigens and indirectly lead to neutralization through enhanced phagocytosis elicited by macrophages, neutrophils, dendritic cells and/or natural killer (NK) cells [22]. Antigenic peptides derived from pathogens (viruses and bacteria) ingested by phagocytic cells are presented in association with Major Histocompatibility Complex (MHC) class II molecules to cognate T- and B-lymphocytes which ultimately results in the clonal selection and proliferation of antigen-specific, antibody-secreting B-lymphocytes [23, 24]

Once bound to the appropriate antigen the B lymphocytes differentiate, producing memory B cells as well as antibody secreting plasma clones which generate antibodies that will recognize the identical antigenic epitope that associated with the antigen receptor [24]. The memory B cells produced during the immune response remain dormant until they are activated by their particular antigen, enhancing the antibody response when re-exposed to a specific antigen [24]. Monoclonal antibodies (mAbs) are produced by a single B lymphocyte clone which recognizes a specific antigenic epitope, whereas polyclonal antibodies are produced by a myriad of proliferating lymphocytes, recognizing numerous antigenic epitopes [24]. The electrophoretic mobility of antibodies usually places them in the γ-globulin fraction of serum. Antibodies, often referred to as immunoglobulins (Ig) are made up of four polypeptides or chains with a molecular weight of ~150 kDa in total [24]. Two identical copies of a heavy (~55 kDa) and light (~25 kDa) chain held together by disulfide and non-covalent bonds make a Y-shaped Ig [25]. The light chains can consist of one of the two types; lambda (l) and kappa (k). The variable (V) regions of both the heavy and light chains cover approximately the first 110 amino acids of each chain, forming the antigen-binding (Fab) regions, while the remaining sequences are constant (C) regions, forming the Fc (fragment crystallizable) regions for effector ligand recognition and binding (Figure 2) [24].

In mammals, there are five classes of Ig; IgG, IgM, IgA, IgD, and IgE, these classes differ in antigenicity, size, function and charge [24].

IgG antibodies can be further categorized into subclasses; IgG1, IgG2, IgG3 and IgG4 with IgG1 being the most abundant antibody present in the human body [26]. IgG antibodies share 90 % similarity in amino acid levels but each subclass responds to different types of antigens [27]. The IgG1 antibody response is stimulated primarily by soluble protein antigens and membrane proteins [28]. Bacterial capsular polysaccharide antigens trigger IgG2 antibody responses [28] and IgG3 can be attributed to being a pro-inflammatory antibody [27]. IgG4 antibody responses can be triggered by allergens and are often expressed following repeated, long term exposure to antigens in a non-infectious situation such as individuals allergic to bees or long-term bee keepers that underwent immune therapy [29, 30].

Antibody diversity is a function of hyper-variable sequences within the variable domains known as the complementarity-determining regions (CDRs), which are responsible for antigen-binding specificities [31]. Both the variable regions of the light and heavy chains consist of 6 CDRs; known as CDR L1 to L6 and CDR H1 to H6 respectively [31]. The 6 CDR sequences in the variable domains of Ig molecules are believed to act synergistically to enable specific antigen recognition; CDR H3 is thought to be the largest surface area of antigen recognition whereas the other CDRs are said to be involved in enhanced binding affinity to the antigen [32]. The genetic diversity of CDR1 and CDR2 are encoded by the germline and are further adapted by somatic mutation [31]. The CDRL3 and CDRH3 however, originate from somatic rearrangement of the variable region [31].

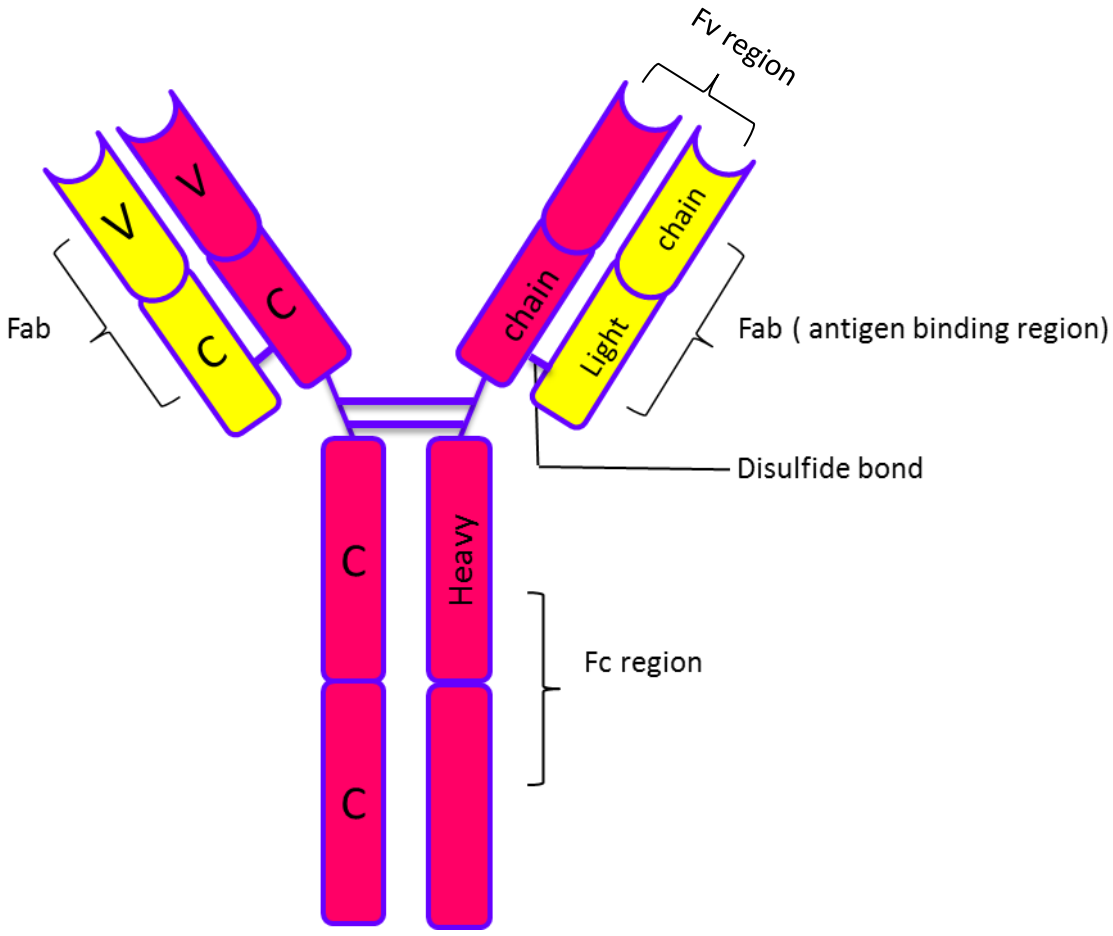

Figure 2. Structural schematic of an antibody:

The Ig is made of two identical heavy (pink) and light (yellow) chains. The chains are linked by disulfide bonds and consist of constant (C) and variable (V) regions. The effector domain, Fc, forms the stem of the antibody while the antigen binding region, known as the Fab fragment, is found at the top of the antibody. The variable heavy (V_H) and variable light (V_L) chains are referred to as the Fv region. The Fab fragment comprises the variable regions of both the heavy and light chains.

A genetically diverse antibody repertoire is the key component in humoral immunity and is vital to the development of a functional adaptive immune response [33]. The primary antibody repertoire is formed during early development through the re-arrangement of programmed gene segments mediated by the recombination activation gene (RAG) [33, 34]. Upon antigen recognition, diversification and maturation of the antibody response occurs giving rise to the secondary antibody repertoire [33, 34]. Recombination and somatic hypermutation are the two main mechanisms responsible for the diversity of the secondary antibody repertoire, primarily targeting regions within the complementarity-determining region (CDR) of the antibody [33]. Recombination involves the re-arrangement of the variable (V), diversity (D) and joining (J) genes of antibodies resulting in an almost limitless sequence diversity within the antibody repertoire [33, 35, 36].

In humans, somatic hypermutation is the primary mechanism of diversification of the secondary antibody repertoire in response to antigenic stimuli [33, 37]. Upon recognition of infecting particles, naïve B-cells undergo somatic hypermutation by mutating the V regions of the antibody genes [38]. These single base mutations usually have no effect on antigen recognition, some mutations even exhibit deleterious effects on either proper folding of the antibody protein or antigen recognition [33]. However, some mutations produced through somatic hypermutation result in enhanced affinity to pathogenic epitopes, consequently providing a platform for the positive selection of high affinity antibodies, characteristic of a mature immune response [39, 40].

1.4.1 mAb derivatives

Fab fragments, a derivative of mAbs comprising of the antigen binding region (Figure 2) are used in biopharmaceutical research and diagnostics and are particularly beneficial in the analysis of antigen-antibody interactions [41]. Fabs are conventionally produced through the enzymatic

digestion of a bivalent mAb by either papain or pepsin [42]. The digested Fab fragments are then purified from the digestion mix; a number of techniques may be employed such as affinity chromatography with either protein A or protein G, ion exchange chromatography, antigen affinity chromatography or size exclusion chromatography [41]. The other widely used approach to producing Fab fragments is transient expression of the light and heavy chain of the fragment in mammalian cell lines; the two peptides are required to assemble simultaneously and are joined by an inter-chain disulfide bond to comprise the Fab fragment [41].

An antibody derivative apart from the Fab fragment that is clinically useful and commercially available is the single-chain Fv fragment (scFv) [43]. These scFv fragments are noncovalent peptides, of ~25-30 kDa, made up of the variable heavy and variable light chain of an antibody, stabilized by a hydrophilic flexible peptide linker between 10 to 12 residues long [43, 44].

1.4.2 Monoclonal antibodies used in biopharmaceutical applications and therapies

Since their introduction into the market in 1986, bioprocessing technology for therapeutic mAb production has greatly advanced [45]. Due to the commercial success of mAbs, substantial investment in research and development by both industry and academia has been attracted [46]. The heightened interest in antibody therapy has resulted in the evolution of detailed mAb engineering techniques that have enabled successful application of antibodies and fragments thereof in many therapeutic areas [46]. MAbs constitute the largest single class of biological drugs under development where mAbs secured 8 of the top 20 spots for best-selling biotechnology drugs in 2007 [47]. All protective antibodies that have been developed in response to vaccines inhibit or clear pathogenic infection, these antibodies are directed to constant or invariant molecular components on the pathogen [48].

1.4.2.1 mAb therapy used in the treatment of cancer

This mAb therapy has also been applied to the treatment of cancer [49]. Human cancer cells express unique surface antigens, which represent a diverse spectrum of targets that are overexpressed, selectively expressed or mutated compared with normal cells [49]. Identifying suitable antigens for antibody-based therapeutics has been the main challenge and molecular techniques allowing the alteration of effector functions, pharmacokinetics, size and immunogenicity of the antibody have emerged as key elements in the development of mAb-based therapies [49]. Oncological mAb therapies function through modulating the immune system by altering T cell activation for example, or through altering receptor or antigen function [50]. Tumor cell killing by mAbs involve several mechanisms, some of which include; induction of apoptosis by direct action of the mAb or immune-mediated cell killing mechanisms such as complement-dependent cytotoxicity (CDC) or antibody-dependent cellular cytotoxicity (ADCC) [49]. The US- Food and Drug Administration (FDA) has approved approximately 12 antibodies for the treatment of various solid tumors and hematological malignancies [49]. Some of these include Trastuzumab, a humanized IgG1 mAb for the treatment of breast cancer, Bevacizumab, also a humanized IgG1 mAb used in first and second line treatment of metastatic colon cancer and Brentuximab vedotin, a chimeric IgG1 mAb used for treatment of relapsed Hodgkin's Lymphoma [49].

1.4.2.2 The market of mAbs targeting autoimmune conditions

Since 2013 the sales and product approval of mAb products has significantly increased, with approximately four to five new mAb approvals each year [51]. The global sales revenue for therapeutic mAb products in 2013 was around $75 million which constitutes around fifty percent of the total sales of all biopharmaceutical products [51]. As of May 2016, 62 therapeutic mAbs have been approved by the FDA, some approved in 2015 include mAbs such as Nivolumab, a programmed death receptor-1 blocking antibody used in the treatment of severe plaque psoriasis, Deratumumab, a mAb that induces apoptosis in CD38 expressing tumour cells for the

treatment of multiple myeloma and Mepolizumab, an interleukin-5 antagonist used in the treatment of severe asthma [52]. MAbs used in the treatment of autoimmune disorders and cancer are the two largest focus areas and comprise almost 85 % of mAbs that are currently marketed [53]. There are approximately 20 commercially available mAbs used in cancer therapy and 21 commercially available mAbs used in the treatment of autoimmune disorders, some of which include; Crohn's disease, psoriasis, asthma, multiple sclerosis, rheumatoid arthritis and osteoporosis [53]. Autoimmune disorders and cancer still seem to be receiving the most development attention with 25 and 22 new mAbs in phase 3 clinical trials, respectively [53]. Monoclonal antibody products will continue to dominate as the major class of biopharmaceutical products as the rate of approved mAbs increases each year [51, 53].

1.4.2.3 Antibodies used in HIV Vaccine therapy

A vaccine that can be used to target HIV-1 would need to elicit antibodies that target a large number of fast evolving highly diverse viral strains, since the amino acid sequences of envelope spikes can differ by as much as >35 % [54]. Consequently, high affinity antibodies that are able to penetrate the glycan shield and bind effectively to highly diversified spikes are needed [48]. Among infected individuals 2 to 4 years post infection, approximately 10 – 30 % develops antibodies with the ability to neutralize a broad range of viral isolates [55]. Of this small fraction <1 % exhibit exceptional cross clade activity and are referred to as broadly neutralizing antibodies (bNAbs) [56].

Until recently, characterizing and identifying mAbs was difficult due to the few techniques available at the time. Despite this, several bNAbs against HIV-1 were identified; while the first neutralizing antibodies (NAbs) identified were not very potent, they did provide insights into the regions of Env that were susceptible to antibody-mediated neutralization [48]. The four conserved sites include the CD4 binding site (CD4bs), the primary receptor for viral entry; the Asn160 glycan-dependent site associated with the hypervariable domain V1 and V2; the Asn332

glycan-dependent site at the base of the V3 loop and the membrane proximal external region (MPER) on gp41 [57] (refer to Figure 3).

In recent times three additional bNAbs that target regions outside the four conserved domains have been described, these include PGT151, 35O22 and 8ANC195 [58-60]. The epitope of the newly described PGT151 mAb comprises of residues and glycans at the interface of gp41 and gp120 and binding of this mAb is dependent on a properly formed, cleaved Env trimer [61]. 35O22 is a potent HIV-mAb that binds a conserved region which spans across gp120 and gp41, the binding specificity of 35O22 represents a novel site of vulnerability on HIV-1 Env commonly stimulated by natural infection [58]. 8ANC195 was the first anti HIV bNAb that bound to an epitope spanning both the gp120 and gp41 subunits [59]. The neutralizing epitope comprises of *N*-linked glycans adjacent to the CD4bs on gp120 and regions on the gp41 subunit [59]. Another group of researchers have also elaborated on an epitope for the previously described, related antibodies 3BC176 and 3BC315, making this epitope distinct from the four well-established target sites [62]. Analysis of the bNAbs indicate that the target site is at the gp41-gp41 inter-subunit interface of the Env trimer in the pre-fusion conformation [62]. This epitope partially overlaps that of 35O22 but both bNAbs have a distinct angle of approach [62].

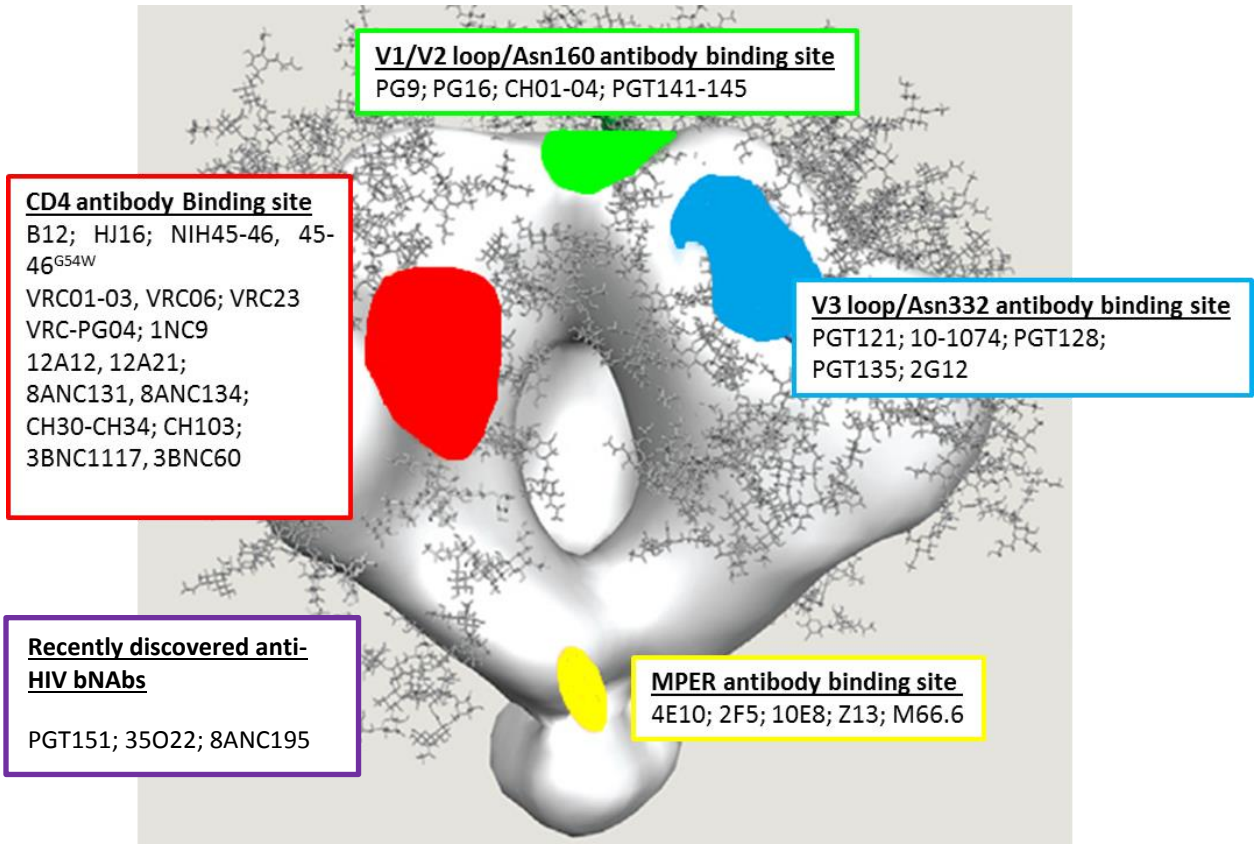

Figure 3.Broadly neutralizing antibodies that target the HIV Env spikes:

An Electron microscopy image of HIV-1 Env trimer with antibody epitopes highlighted on the surface of the structure. There are 4 main epitopes highlighted; the CD4 binding site epitope (red), MPER binding site (yellow), V3 loop/Asn332 binding site (blue) and V1/V2 loop/Asn160 binding site (green). In recent times 3 newly discovered bNAbs outside the 4 conserved domains have been described, the target site is at the interface of gp120-gp41 these include, PGT151, 35O22 and 8ANC195 (purple) (Adapted from [48, 63]).

Despite being a well-protected, buried region on the HIV Env spike that is highly conserved, the CD4bs is accessible to both CD4 receptors and CD4bs antibodies (Figure 3) [48, 64]. Of those that target the CD4bs, NIH45-46 and 3BNC117 are the most potent antibodies [48, 65]. Structural analysis of the antibodies reveal that even though they were isolated from different individuals, antibodies derived from the variable heavy chain (VH)-gene segment VH1-2 share a common mode of antigen recognition whereby framework residues contribute to CD4 mimicry [48, 66, 67] [64, 68]. CD4 bNAbs are able to bind to the CD4bs when a short complementarity-determining region 3 of the light chain (CDR L3) interacts with the gp120 V5 and the gp120 diversity (D) loops, as a short CDR L1 avoids clashes with glycans at Asn^{276} on the D loop [64, 66-68]. This mechanism allows these anti-CD4bs antibodies to compete for binding at the CD4bs on the viral gp120 Env, thereby inhibiting cell entry [48].

Despite the myriad of anti-HIV therapies that have been described and implemented as part of a treatment regimen, without a *bona fide* cure the need to develop and discover new and improved approaches to combatting HIV is still an important, continuing research objective. One such agent that is being explored is the anti-CD4 monoclonal antibody, Ibalizumab.

1.5 The anti-CD4 monoclonal antibody: Ibalizumab

Ibalizumab (previously known as Hu5A8 and TNX-355) is a humanized IgG4 anti-CD4 mAb that mediates potent anti-HIV activity [69]. CD4 is a 55 kDa host cell surface glycoprotein composed of four immunoglobin-like domains (D1-D4) expressed on a subset of T lymphocytes, it also consists of a membrane spanning domain and a cytoplasmic tail which interacts with src-like tyrosine kinase [70, 71]. The amino acid sequence of D1 shares similarities with that of variable regions of immunoglobulins [72]. CD4 utilizes MHC class II molecules as a restriction element for antigen recognition and functions to enhance T-cell receptor (TCR)-mediated signaling [70]. MHC class II molecules are vital for the initiation of the antigen-specific immune response, as their

main function is to present processed antigens, primarily derived from exogenous sources such as bacterial or viral particles, to $CD4^+$ T-lymphocytes [70]. CD4 associates directly with MHC II molecules, on antigen-presenting cells, which triggers the recruitment of a tyrosine kinase, $p56^{lck}$ on the $CD4^+$ T-lymphocytes. This interaction mediates the activation of helper T cells thereby moderating the adaptive immune response [73]. Therefore, disruption of MHC antigen presentation directly affects immune responses to infection.

Ibalizumab was generated by immunization of BALB/c mice with $CD4^+$ CHO cell transfectants which were stably expressing full length human CD4 [69]. The anti-CD4 mAbs that were generated during this study were tested for their ability to cross-inhibit other anti-CD4 mAbs allowing the identification of mAbs that recognize spatially proximal or distinct epitopes on CD4 [69]. Ibalizumab was distinguished by its failure to compete with neither the two D1-specific mAbs, Leu 3A and OKT4a nor with OKT4, the D3/D4-specific mAb [69]. The data obtained in this study suggested that Ibalizumab recognized a distinct epitope on CD4 from those defined by several other D1- and D3/D4-specific mAbs [69].

Ibalizumab binds to the interface between domain 1 and 2 of CD4, away from the binding site of MHC class II molecules [74] (Figure 4). Moreover, all conformational changes induced by Ibalizumab appear to be localized, primarily making contact with the BC loop at the junction of D1 and D2 of CD4 located on the opposite end of the MHC II and gp120 binding sites [75]. There are minor, local conformational changes that occur at the binding interface of CD4 and Ibalizumab, these slight changes do not extend to other regions of CD4 likely explaining why this antibody does not interfere with CD4 receptor function [75, 76]. The anti-CD4 mAb inhibits CD4-dependent virus entry and is able to inhibit a broad range of HIV isolates including R5, X4 and R5X4 strains.

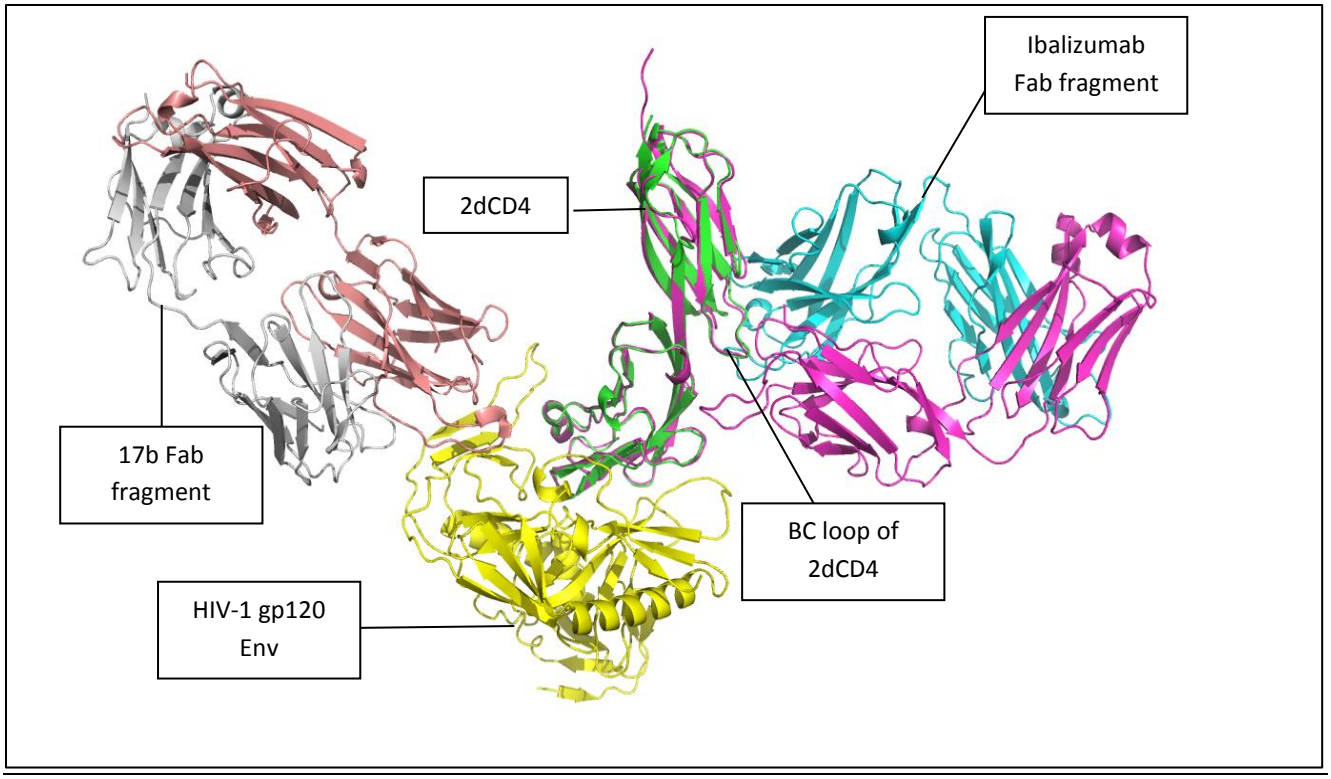

Figure 4. Three-dimensional structure of a complex of 2dCD4, the Fab fragment of Ibalizumab, gp120 and the Fab fragment of 17b (obtained through structural alignment of the Ibalizumab Fab fragment and gp120 associated with 2dCD4)

Side view of the Fab fragment of Ibalizumab and 2dCD4 in complex with gp120 and the Fab fragment of 17b. 2dCD4 is in light green and magenta, the heavy chain of Ibalizumab in blue and the light chain in magenta. gp120 is in yellow, the heavy chain of 17b in salmon and the light chain in grey. The BC loop in D2 of CD4, constituting the core epitope of Ibalizumab are indicated. The diagram illustrates the distinct epitopes of Ibalizumab and gp120 to 2dCD4. The two binding sites of gp120 and Ibalizumab do not cause any steric hindrance to each other. gp120 binding is not affected by Ibalizumab binding to CD4 nor are any gp120-induced epitopes masked by this mAb. Diagram rendered using PyMOL (PyMOL Molecular Graphics System, Version 1.8 Schrödinger, LLC) and pdb files 1G9M and 3O2D.

Phase II clinical trials have shown that Ibalizumab is well tolerated at therapeutic doses that achieve significant and sustained reductions in viral loads in treatment experienced HIV positive individuals failing standard therapy [17, 77, 78]. There were three main studies conducted on Ibalizumab which illustrate reductions in plasma HIV-1 RNA levels by > 1 $\log_{10}$ copies/ml in HIV infected patients [17, 77, 78] (Table 1).

Table 1. Summary of reduction in viral loads as observed in Ibalizumab clinical trials

Study	Dose (mg/kg)	Reduction in Viral RNA levels (copies/ml)
1. Antiretroviral Activity of the Anti-CD4 Monoclonal Antibody TNX-355 in Patients Infected with HIV Type 1 **[77]**	3.0 mg/kg, 10 mg/kg, and 25 mg/kg	0.56, 1.33, and 1.11 $\log_{10}$
2. Safety, Pharmacokinetics, and Antiretroviral Activity of Multiple Doses of Ibalizumab (formerly TNX-355), an Anti-CD4 Monoclonal Antibody, in Human Immunodeficiency Virus Type 1-Infected Adults [17]	Arm A – 10mg/kg (weekly for 9 weeks) Arm B – 10mg/kg (initially), 6mg/kg (after 2 weeks) Arm C – 25mg/kg (every 2 weeks for 8 weeks)	0.5 to 1.7 log10 Complete coating in arm B was not achieved after two weeks
3. Phase 2 efficacy and safety of the novel entry inhibitor, TNX-355, in combination with optimized background regimen (OBR). **[79]**	10mg/kg (weekly for 8 weeks),10mg/kg (every 2 weeks), and 15mg/kg (every 2 weeks)	0.95 to 1.16 log10

In contrast to other entry inhibitors that target gp120, the interaction between gp120 and CD4 is not inhibited by ibalizumab; alternatively this mAb acts as an antiviral agent by preventing the interaction of CD4-bound gp120 with its co-receptors (CCR5 and/or CXCR4), via a mechanism thought to involve impedance of required structural rearrangements in the receptor complex [69] (Figure 4). Other anti-CD4 antibodies that bind domain 1 of CD4 and inhibit gp120 attachment, have been found to be immunosuppressive, as they inhibit the function of MHC II peptides, and are not suitable for the treatment of HIV infection [76]. Immunosuppression occurs through competitive binding with MHC class II molecules, and adversely affects CD4-dependent

antigen presentation [80]. Conversely, Ibalizumab has shown no immunosuppressive effects in human trials, as it does not obstruct MHC II binding sites, and is an excellent candidate for anti-viral therapy [76].

Recently, bispecific antibodies (biNAb) were designed that combined the HIV inhibitory properties of Ibalizumab and gp120 specific bNAbs [81]. Two biNAbs that were created PG9-Ibalizumab and PG16-Ibalizumab exhibited remarkable breadth and efficacy, and were able to neutralize 100 % of the 118 viruses tested at low picomolar concentrations. The mechanism behind the neutralization of this biNAb lies with the synergistic activity of both PG9 and Ibalizumab, an activity that is thought to be enhanced by the flexibility of the scFv fragment of PG9 on the biNAb molecule [81]. This study proposed that potent biNAbs such as the ones created should be considered as passive immunization agents against HIV-1. Thus far, these biNAbs are the only antibody-like molecules that are able to inhibit all viruses tested. Neutralization by PG9-Ibalizumab and PG16-Ibalizumab is more efficient than any other antibody described, including NIH45-46^{G54W} [66, 81].

While the broad-ranging therapeutic effects of Ibalizumab are impressive, the costs of sufficient antibody production hinder further development for clinical use. The reduced complexity and simple structure of Fab fragments compared to full antibodies allows for production in microbial cells, which is often attractive due to the rapid growth of prokaryotic expression systems [82]. The use of microbial expression vectors is cost effective and antibody derivatives show improved specificity along with therapeutic efficiency [82]. Antibody fragments exhibit superior tissue penetration compared to full antibodies and their reduced complexity allows the retention of specificity and affinity for their targets [82].

While there are well-documented challenges associated with the expression of functional Fab fragments in *E. coli*, largely related to chain folding and assembly, several of these types of

molecules have been produced successfully in bacterial expression systems and their clinical use is now well-established. Examples include ReoPro (abciximab), a platelet membrane glycoprotein IIb/IIIa receptor inhibitor used for the treatment of patients undergoing high-risk percutaneous coronary interventions, DigiFab, (digoxin immune Fab), used for the treatment of digoxin intoxication [83] and Crotiladae Polyvalent Immune Fab, (CroFab), a polyvalent bovine-derived antivenom [84]. Building on from this, this study investigated the feasibility of producing a functional Ibalizumab Fab fragment in *E. coli,* and evaluated the efficacy of this molecule as a potential antiviral therapy.

1.6 Aim and Objectives

The overall aim of this study was to purify and reconstitute a functional Fab fragment of Ibalizumab following expression in *E. coli*.

This was achieved by carrying out the following specific objectives:

a. To design and synthesize codon-optimized sequences encoding the Heavy and Light chains of the Ibalizumab Fab region comprising variable (VH/VL) and constant (CH1/CL) domains;
b. To clone these fragments into the prokaryotic pET15b expression vector;
c. To optimize bicistronic expression of the heavy chain (VHCH1, henceforth designated $IBLZ_H$) and light chain (VLCL, henceforth designated $IBLZ_L$) sequences in BL21 *Escherichia coli* cells;
d. To extract a functional Ibalizumab Fab fragment ($IBLZ_{Fab}$) from the bacterial periplasm
e. To purify $IBLZ_{Fab}$ by affinity chromatography procedures;
f. To analyze the CD4-binding properties of $IBLZ_{Fab}$ by Surface Plasmon Resonance (SPR).
g. To analyze the CD4-binding properties of $IBLZ_{Fab}$ by Enzyme-linked Immunosorbent Assays (ELISA)
h. To analyze the neutralization properties of the $IBLZ_{Fab}$ by Neutralization assays using a psuedovirion inhibition assay.

2 Chapter 2: Experimental procedures

For expression of the Ibalizumab Fab regions, a bicistronic cassette was designed where both the light and heavy chain contained an OmpA (Outer-Membrane Protein A) leader sequence. The DNA encoding the variable and constant heavy chains, and the variable and constant light chains were separated by an inter-cistronic ribosomal binding site.

Typically for IgG expression in mammalian cell lines, two different genes are transfected into a cell for stable expression, this can either be achieved by co-transfection of the genes or by designing a bicistronic expression vector [85]. However, the latter may be applied to Gram negative bacterial expression of antibody derivatives [86]. The inter-cistronic ribosomal binding site located between the heavy and light chains allows successful co-translation of the two cistrons on the same construct [87].

2.1 Cloning of $IBLZ_{Fab}$ expression cassettes

DNA cassettes encoding the heavy and light chains of the Ibalizumab Fab region were synthesized following codon optimization for expression in *E. coli* (GeneArt, Germany, Appendix 2). The cassettes contained 5'- and 3'-restriction endonuclease sequences (*Nco*I and *Xho*I respectively), an ompA signal sequence and encode an N-terminal 6x histidine tag to facilitate purification of $IBLZ_{Fab}$ by affinity chromatography (Figure 5).

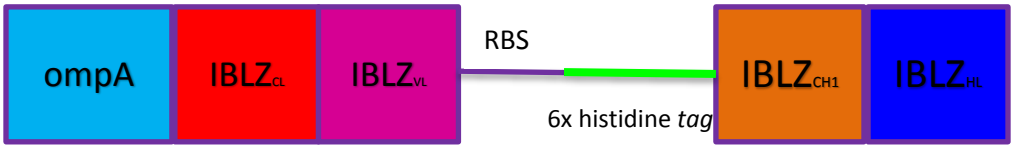

Figure 5. Schematic representation of the bacterial IBLZ Fab ($IBLZ_{fab}$) expression cassette:

The cassettes comprised of 5'- and 3'-restriction endonuclease sequences (*Bsp*HI and *Xho*I, respectively) for subcloning of the Fab fragment into pET15b; this includes the constant heavy chain 1, variable heavy chain, constant light chain and variable light chain in addition to the leader sequence OmpA required for periplasmic transport. The variable light and heavy chains were inserted as a complete construct together with the intercistronic ribosomal binding site (RBS).

2.1.1 Preparation of $IBLZ_{Fab}$-Encoding DNA for subcloning (Digestion and ligation of pET15b plasmid vector and $IBLZ_{Fab}$ Fragment)

The pET15b vector DNA and the pMK-RQ plasmid containing the $IBLZ_{Fab}$ encoding DNA (GeneArt, Germany) was digested with the restriction endonucleases *Xho*I and *Nco*I (Fermentas; Canada) and *Bsp*HI and *Xho*I respectively. Restriction reactions contained *Xho*I (20 U), *Nco*I/*Bsp*HI (20 U), 1 x Fast Digest buffer and either pET15b or pMK-RQ DNA (3 µg) and were incubated at 37˚C for 1 hour. The resulting fragments were resolved on a 0.8 % agarose gel and the bicistronic $IBLZ_{Fab}$-encoding DNA was excised and purified using a MinElute Gel Extraction Kit (Qiagen; Germany), according to the maufacturer's instructions. The concentration of the purified bicistronic $IBLZ_{Fab}$ DNA was measured spectrophotometrically at 260 nm (Nanodrop Technologies Inc; US) and used in ligation reactions. Ligation reactions were performed using a T4 DNA Ligase Kit (Fermentas; Canada). The reaction contained T4 DNA Ligase (1 U), 1 x T4 DNA Ligase buffer, pET15b vector DNA (50 ng) (Novagen, US) and $IBLZ_{Fab}$ insert DNA (50 ng). The reaction was incubated at 20˚C for 4-6 hours. Competent DH5α *E. coli* were then transformed with 5µl of the ligation mix was then used to transform competent DH5α *E. coli* bacterial cells.

Colonies visible on positive ligation agar plates were selected under sterile conditions and cultured in 10 ml Luria-Bertani (LB) broth containing ampicillin (100 µg/ml). Cultures were incubated at 37˚C overnight in an orbital shaker (250 rpm).

Recombinant plasmids were isolated from overnight cultures using a Sigma GenElute™ Plasmid Miniprep Kit (Sigma-Aldrich; Germany), according to the manufacturer's instructions. Screening for positive clones was performed by restriction mapping analysis. The pET15b-IBLZ$_{Fab}$ construct was linearized with *Xho*I and *Bam*HI respectively (Fermentas; Canada), in order to obtain an estimation of the size of the plasmid containing the insert. A double digestion with *Xho*I and *Nco*I as well as *Xho*I and *Xba*I were performed to excise the IBLZ$_{Fab}$-encoding DNA fragment from the recombinant pET15b vector. All digestion reactions were incubated at 37˚C for 1 hour. Digested products and controls (undigested and linearized plasmid including plasmid containing no insert) were resolved on a 1 % agarose gel and visualized in a Universal Hood Gel Doc instrument (Bio-Rad; US) under UV light.

In order to confirm the IBLZ$_{Fab}$ coding sequence in the pET15b-IBLZ$_{Fab}$ constructs Sanger sequencing was performed. T7 promoter and terminator primers were used during PCR reactions in order to amplify the IBLZ$_{Fab}$ sequence within the pET15b vector. Cycling conditions were as follows: an initial hotstart denaturation at 94˚C for 2 minutes was followed by 40 cycles with each cycle comprising denaturation at 94˚C for 1 minute, annealing at 50˚C for 30 seconds and elongation at 72˚C for 6 minutes. Once the cycles were complete, a final extension at 68˚C for 10 minutes was applied. The reaction was cooled to 4˚C and maintained at this temperature until analyzed by agarose gel electrophoresis. Subsequent to gel analysis on a 1 % agarose gel the PCR reactions were purified using a GeneJet PCR Purification Kit (Thermo Fisher Scientific, US) as per the manufacturer's instructions. A second cycling sequencing PCR reaction was performed which included fluorescent labeling of the DNA bases, allowing the sequence to be read. The PCR amplicon of the plasmid insert was sequenced using ABI cycle sequencing with an ABI 3730 DNA Analyzer. Sequences were viewed with the Sequencher™ v.5.1 software and the sequences were

compared with the DNA cassettes encoding the heavy and light chains of the Ibalizumab Fab region from GeneArt.

2.2 Expression of the IBLZ$_{Fab}$ fragment in Bacterial Cell Culture

Recombinant pET15-IBLZ$_{Fab}$ vectors were used to transform BL21 Star^{TM} (DE3) *E. coli* (Thermo Fisher Scientific, US) under sterile conditions (see appendix for transformation procedure). Transformed *E. coli* cells were spread onto agar plates, containing ampicillin (100 µg/ml) and incubated at 37˚C overnight. A single colony was then selected and used to inoculate two 1 L Erlenmeyer flasks containing 250 ml of LB Broth supplemented with ampicillin (100 µg/ml). The cultures were incubated at 37˚C in an orbital shaker (250 rpm) overnight.

The next day, 50 ml of overnight culture was added to 1 L of LB Broth supplemented with ampicillin (100 µg/ml). A total of 8 L of LB Broth was prepared and incubated at 37˚C in an orbital shaker (250 rpm) for approximately 5 hours or until the A_{600} reached 0.6 (mid log growth phase). The cultures were then incubated overnight at 30˚C in an orbital shaker (200 rpm) to induce over expression of the Fab fragment.

2.3 Extraction and Purification of IBLZ$_{Fab}$

2.3.1 Extraction of protein expression

Cultures expressing IBLZ$_{Fab}$ fragments were harvested by centrifugation (2000 x *g* for 20 minutes). The supernatant was discarded and the cell pellet washed with 1 x PBS Buffer (Phosphate Buffered Saline, pH 7.4, 30 ml/L of overnight expression culture pellet) to remove any excess LB broth. The washed cell pellet was harvested once more by centrifugation (2000 x *g* for 20

minutes). Each cell pellet obtained from 1 liter of LB broth was then treated with 250 ml of sucrose buffer (200mM tris(hydroxymethyl)aminomethane (Tris), 20 % sucrose and 1mM Ethylenediaminetetraacetic acid (EDTA), and 0.5 mg/ml of chicken lysozyme (Sigma-Aldrich; Germany) for 1 hour on ice with gentle agitation. One volume, 250 ml, of sterile distilled water was then added and the suspension agitated on ice for a further hour. The periplasmic fraction containing $IBLZ_{Fab}$ was recovered by centrifugation (10 000 x *g*, for 25 minutes).

2.3.2 Purification procedure of $IBLZ_{Fab}$

Purification of the recombinant $IBLZ_{Fab}$ fragment was achieved by affinity chromatography using a kappa specific matrix (Capture Select Kappa Matrix (Life Technologies; US) which associated with the kappa light chain of $IBLZ_{Fab}$.

A total volume of 5 ml packed kappa specific agarose was added to the lysates (4 L) and incubated at 4˚C overnight with gentle stirring. The next morning the incubated beads were collected using an End fitting w/Fixed 10 µM Pyrex® Frit column (Sigma-Aldrich; Germany). The resin was then incubated with 15 ml of 20 mM Citric Acid and 1 M Sodium Chloride (pH 3.5) solution for one hour on ice with gentle stirring and thereafter collected. Samples (100 µl) were collected from the total cell sample, periplasmic fraction, unbound protein and elution for analysis by reducing and non-reducing SDS-PAGE (12.5 % gels) and western blot for the presence or absence of bands corresponding to $IBLZ_{Fab}$ using standard techniques [88].

For western blotting, proteins were transferred from SDS-PAGE gels onto Hybond-C nitrocellulose membrane (Bio-Rad; US) using a Trans-Blot SD Semi-Dry Transfer Cell System (Bio-Rad; US) at 20 volts for 30 minutes. Thereafter, the membrane was blocked with 5 % fat free milk powder in Tris-buffered saline containing 0.1 % Tween-20 (T-TBS) for 1 hour at room temperature with gentle agitation. The membrane was then probed with a horseradish peroxidase (HRP)-

conjugated monoclonal antibody to human Kappa light chain (Abcam®; UK) at a dilution of 1 in 500 (details outlined in Appendix 1). The high background visible in western blot images could be attributed to a number of factors; high antibody concentration, the presence of excess SDS on the blot and even the exposure time of the antibody to the blot. Various concentrations were tested during western blot analysis and the concentration of 1 in 500 gave optimum detection. Detection of $IBLZ_{Fab}$ was performed by standard chemiluminescence methods and viewed using a Universal Hood Gel Doc instrument (Bio-Rad; US).

The eluted protein was concentrated using an Amicon® Ultra-15 Centrifugal filter device (molecular weight cut off at 10 kDa) (Millipore; US), according to the manufacturer's instructions (2 500 x *g*, for 12 minutes – repeated until 2 ml was obtained). The total protein concentration was determined using the BCA assay kit, (Thermo Fisher Scientific; US) (See Appendix 1 for procedure).

This was then applied to a Sephadex G-75 AKTA-FPLC P-920 column (GE-Healthcare; UK) pre-equilibrated with 1 x PBS, and separated at a flow rate of 1 ml/minute. Fraction volumes of 3 ml were collected and fractions within a single peak were and concentrated in an Amicon® Ultra-15 Centrifugal filter device (Millipore; US) (molecular weight cut off at 10 kDa) before being electrophoretically separated using SDS-PAGE and Coomassie staining. A total of 30 μl of sample was added to each well and all sample concentrations were normalized for analysis. Expression and purification procedures of $IBLZ_{Fab}$ were replicated and reproducibility of results were achieved.

2.4 Expression and Purification of 2 domain CD4 (2dCD4)

Recombinant pET15-2dCD4 vectors (Novagen, US) (cloned in house), were used to transform BL21 Star™ (DE3) *E. coli* (Thermo Fisher Scientific, US) under sterile conditions [89]. The agar plates, containing ampicillin (100 µg/ml) were incubated at 37˚C overnight. A single colony was then selected and used to inoculate four 50 ml Falcon centrifuge tubes containing 20 ml of LB Broth and ampicillin (100 µg/ml). The cultures were incubated at 37˚C in an orbital shaker (250 rpm) overnight.

The next day, 20 ml of overnight culture was added to 1 L of LB broth supplemented with ampicillin (100 µg/ml). A total of 4 L of LB Broth was prepared and incubated at 37˚C in an orbital shaker (250 rpm) to induce log phase growth for approximately 5 hours or until the A_{600} reached 0.6 (mid log growth phase). The cultures were then incubated overnight at 20˚C in an orbital shaker (200 rpm) to induce over expression of the 2dCD4 protein.

2.4.1 Purification of 2dCD4

The 6x histidine tagged 2dCD4 expressing *E. coli* was collected by centrifugation at 2 000 x *g* for 20 minutes. The cell pellet collected from 1 L of expression media was re-suspended in 25 ml of PBS, pH 7.4 containing 0.5 mg/ml of chicken lysozyme (53,000 units/mg, Sigma-Aldrich; Germany). The cell suspension was incubated at 4˚C for 1 hour with gentle stirring, and snap-frozen in dry-ice and acetone. Complete lysis was effected by 2 cycles of freeze-thawing followed by sonication on ice for 3-4 cycles of 1 minute pulses, at an amplitude of 80 %, pulse on for 1 second, pulse off for 0.5 seconds (Sonoplus, Germany). The 2dCD4-containing inclusion bodies and other insoluble cell debris were recovered by centrifugation (10 000 x *g*, for 45 minutes). The proteins were then extracted by homogenization using a tissue homogenizer (Omni International, US) in a PBS-based solubilization buffer containing 8 M urea. The homogenate was then centrifuged at 20 000 x *g* for 45 min and the supernatant was purified by standard

immobilized metal-affinity chromatography (IMAC). To prepare the nickel-charged iminodiacetae sepharose 6B resin, two 15 ml falcon tubes containing 2 ml of the resin solution (1 ml resin: 1ml 20 % ethanol) were each washed thrice with 13 ml distilled water (dH_2O) and centrifuged at 1118 x *g* for 5 minutes. To each tube, 10 ml of a 0.1 M $NiSO_4$ solution was added followed by incubation at ambient temperature for 15 minutes with gentle agitation. The tubes were centrifuged as previously described above and the supernatant discarded. The resin was then washed with dH_2O thrice before being applied to pooled lysates and incubated overnight at 4˚C with gentle stirring.

Purification of the 2dCD4 protein was performed using a batch procedure. After the overnight incubation, the beads were centrifuged at 1118 x *g* for 5 minutes and the flow through discarded. The resin was then washed 5 times with 50 ml of wash buffer (50 mM Glycine, 2 mM β-mercaptaethanol and 8 M Urea (pH 7.2)) containing 20 mM imidazole, and thereafter a further 5 times with 50 ml of wash buffer containing 50 mM imidazole. The protein was eluted in 7 ml of wash buffer containing 500 mM imidazole.

Following affinity purification, a reconstituted 2dCD4 was generated by optimized oxidative refolding procedures. The purified, denatured 2dCD4 protein was assembled following stepwise reduction of urea concentration by dialysis in a SnakeSkin® Pleated Dialysis Tubing (Pierce; Rockford, IL). The purified 2dCD4 protein (7 ml) was dialyzed overnight at 4 °C against 1 liter of folding buffer 1 (50mM glycine, 1 mM EDTA, 10 % sucrose, 1 mM reduced GSH, 0.1 mM oxidized glutathione (GSSG) and 4 M urea, adjusted to pH 9.6 with NaOH) and then added into 1 liter of folding buffer 2 (50 mM sodium carbonate, 1 mM EDTA, 10 % sucrose, 0.1 mM GSH, 0.01 mM GSSG, pH 9.6) for a second overnight dialysis at 4 °C with gentle stirring.

This was then followed by exhaustive dialysis against PBS, pH 7.4 (three times with 2 liters, 4 h for the first two dialyses, and then overnight for the final dialysis at 4 °C). The dialyzed protein was then filtered through a 0.45 µm syringe filter, concentrated in an Amicon® Ultra-15 Centrifugal filter device (molecular weight cut off at 10 kDa) (Millipore; Billerica, MA) and stored in aliquots at -80˚C. Samples were collected from the solution at various intervals and analyzed

by reducing and non-reducing SDS-PAGE and western blot analysis and concentration was determined using the Bradford assay (see Appendix 1 for procedure).

2.5 Functionality testing of $IBLZ_{Fab}$

In order to test the functionality of the purified recombinant $IBLZ_{Fab}$ Enzyme-linked Immunosorbent Assays (ELISA), Surface Plasmon Resonance (SPR) and viral inhibition assays were performed.

2.5.1 Enzyme-linked Immunosorbent Assay (ELISA)

Maxisorp microtiter plates (Nunc, Denmark) were coated with 100 µl of 2dCD4 (1 µg/ml) prepared in 1 x PBS solution for one hour. The coating solution containing any unbound protein was then aspirated using an automated BioTek® EL X50 plate washer (BioTek® Instruments, Vermont). The 2dCD4-coated plates were then blocked with 300 µl Bovine Serum Albumin (BSA, 10 mg/ml) prepared in a Phosphate-buffered Saline solution containing 1 x PBS and 0.05 % Tween-20 (PBS-T) overnight at 4˚C. The blocking solution was aspirated and the plate washed with PBS-T thrice. Following this, 100 µl of $IBLZ_{Fab}$ (1 µg/ml) was added to the bound 2dCD4 and incubated for 1 hour at ambient temperature in the dark. The plate was washed five times with PBS-T in order to discard all unbound proteins. Bound $IBLZ_{Fab}$ was detected using 100 µl of a horseradish peroxidase-conjugated monoclonal anti-human kappa light chain antibody (Amersham Biosciences), diluted 1:2000 in PBS-T and incubated for 1 hour at 4 °C. The plate was washed five times with PBS-T and bound $IBLZ_{Fab}$ fragments detected by adding 100 µl of Sure Blue™ TMB Microwell Peroxidase substrate (KPL; Gaithersburg, MD). This reaction was stopped by adding 100 µl of 1 M Sulphuric Acid solution. The absorbance was then read at a wavelength of 450 nm using a Model 680 Micro-plate reader (Bio-Rad; US).

Three main ELISA formats were used, and unliganded 2dCD4 (2dCD4 not associated to any protein complex) was used as a negative control in all ELISA experiments performed. The first involved binding of the periplasmic fraction of $IBLZ_{Fab}$ to 2dCD4, in order to determine whether the Fab fragment of interest was in fact present in the extracted periplasmic fraction. The complex of 2dCD4-$IBLZ_{Fab}$ was detected using horseradish peroxidase-conjugated monoclonal anti-human kappa light chain antibody (Amersham Biosciences, UK).

The second ELISA format analyzed the binding activity of each fraction, after SEC separation, identifying which of the three fractions isolated contained the highest concentration of functional $IBLZ_{Fab}$ fragments. This ELISA involved coating WT 2dCD4 at 1 µg/ml on a 96 well Maxisorp microtiter plate (Nunc, Denmark), followed by binding of $IBLZ_{Fab}$ fractions at varying concentrations, ranging from 1 µM to 0 µM. The complex was detected using an anti-kappa light chain antibody at a concentration of 1:1000. The result of this experiment will not be compromised by the his-tag on the $IBLZ_{Fab}$ since the tag could not be detected using an anti-his probe (See Appendix 3).

The third and final ELISA format assayed the ability of gp120 to bind to 2dCD4 in the presence of the bacterially expressed $IBLZ_{Fab}$ fragment. In addition, this assay aimed to determine the extent of CD4 induced epitope changes in gp120 in the presence of the $IBLZ_{Fab}$ fragment. A 96 well Maxisorp microtiter plate (Nunc, Denmark) was coated with 1 µg/ml of 2dCD4, followed by binding $IBLZ_{Fab}$ at 1 µg/ml and finally allowing gp120 to associate with 2dCD4, gp120-BAL was allowed to bind at varying concentrations ranging from 1 µM to 0 µM. The gp120-2dCD4 complexes were detected using 2G12 and 17b.

Each ELISA assay was performed in triplicate and three biological replicates were obtained for every assay completed. Mean and standard deviation was calculated using Microsoft excel (Windows 7) before evaluating any significant interactions between $IBLZ_{Fab}$ and 2dCD4.

2.5.2 Surface Plasmon Resonance (SPR): Analysis of the 2dCD4-IBLZ$_{Fab}$ interaction

Surface Plasmon Resonance (SPR) was used to determine the kinetics of the 2dCD4-IBLZ$_{Fab}$ interaction. All SPR experiments were performed on a ProteON XPR 36 instrument (BioRad; US). For direct binding comparisons and kinetics, 2dCD4-WT was immobilized on separate flow cells within the same sensor chip using amine coupling according to the manufacturer's instructions. Briefly, a solution of 0.2 M 1-ethyl-3-(3-dimethylaminopropyl) carbodiimide hydrochloride and 0.05 M *N*-hydroxysuccinimide was used to activate carboxyl groups on the sensor surface at a flow rate of 5 µl/min for 10 min. The recombinant 2dCD4 was prepared in a sodium acetate buffer (100 mM, pH 5.5) at a final concentration of 0.1 mg/ml and passed over the activated sensor chip surface at a flow rate of 5 µl/min until the desired immobilization level (2 500 response units) was achieved. Excess carboxyl groups were capped by injection of 1 M ethanolamine, pH 8.0, at a flow rate of 5 µl/min for 5 min. The fraction with the highest 2dCD4 binding activity as measured using ELISA was used in SPR studies. IBLZ$_{Fab}$, pooled fraction 1, was passed over the 2dCD4 surfaces at varying concentrations (from 500 nM to 0 nM) in order to obtain kinetic data. Surfaces with no immobilized protein were used to control for non-specific binding effects. SPR experiments were performed in quadruplicate and reproducibility was achieved. Surface Plasmon Resonance data was analyzed using the ProteOn Manager Software (BioRad; US). Data was fitted to a 1:1 Langmuir binding model.

2.5.3 Viral inhibition: Neutralization assays of IBLZ$_{Fab}$

In order to test the inhibiting properties of the microbially expressed IBLZ$_{Fab}$ *in vitro,* neutralization tests were performed using two pseudoviruses; CAP210 and SF162. The HEK293T and TZM-bl adherent cell lines were sustained in Dulbecco's modified Eagles Medium (DMEM) (Sigma-Aldrich, MO, USA) supplemented with 10 % fetal calf serum (FCS) (Gibco, Life Technologies, US), 2 mM GlutaMax (Gibco, Life Technologies, USA), penicillin (100 units/ml) and streptomycin (0.1 mg/ml) (Sigma-Aldrich, US).

2.5.3.1 Virus amplification

The antiviral efficacy of $IBLZ_{Fab}$ was obtained using an HIV-1 pseudotyped virus neutralizing assay previously described [90]. For the production of HIV-1 pseudoviruses HEK293T cells were co-transfected with Env-deficient backbone expression plasmid (pSG3ΔEnv) and either SF162 LS or CAP210. Polyfect transfection reagent (Qiagen, Hilden, Germany) was used according to the manufacturer's instructions for all transfections that were carried out in a T25 tissue culture flask (Nunc, Roskilde, Denmark). Briefly, 1.2 x 10^6 cells were seeded in a T25 flask 24 hours before transfection. The purified plasmid DNA (8 µg) was added to 40 µl of Polyfect in a final volume of 500 µl of serum free media II (SFMII) (Life Technologies; US), using a ratio of 2:1 (Env: Backbone plasmids). The samples were mixed and allowed to incubate at ambient temperature for 5 minutes before being added to the cells. Twelve hours later the supernatant was removed and 5 ml of complete DMEM was added. The pseudovirus supernatant was harvested 48 hours later by centrifugation at 1 000 x *g*, FCS concentration adjusted to 20 % and thereafter viral supernatants filtered through a 0.2-micron syringe filter. Aliquots were stored at -80˚C.

2.5.3.2 Infectivity determination of Pseudoviruses

According to methods previously described [90] stored aliquots of HIV-1 pseudoviruses were titrated against the TZM-bl cell line in order to determine the Median Tissue Culture Infectious Dosage ($TCID_{50}$). Using a 96 well tissue culture plate (Nunc; Denmark) a five-fold dilution series of each pseudovirus stock was prepared, in complete DMEM in a final volume of 100 µl. Cells were manually counted after being stained by Trypan Blue (Sigma-Aldrich, MO, USA) at a 1:5 ratio with 0.4 % of the trypan blue solution. All viable cells were then enumerated by microscopic inspection of the stained cell suspension using a Neubauer haemocytometer (Roth; Germany). One hundred microliters of 1 × 10^5 cells/ml containing diethylaminoethyl-dextran hydrochloride (DEAE Dextran) in complete DMEM were added to each well. Pseudovirus stocks were titrated four times and a final concentration of 20 µg/ml DEAE Dextran (Sigma-Aldrich, MO, USA) was added to the media. Cells were incubated for an additional 48 hours and infectivity determined

by means of the tat-inducible luciferase-based reporter assay. The cell culture media was aspirated from each well after the 48-hour incubation and the cells lyzed by adding 100 µl of Glo-Lysis buffer (Promega; US). After incubation of lysates at room temperature for 5 minutes, 50 µl of the cell lysate was transferred to a 96-well white solid luminometer plate (Promega, US) to which an equal volume of Bright-Glo™ Luciferase reagent (Promega; WI, USA) was added. The luminescence was quantified using a GloMax® Discover and Explore Detection System (Promega; WI, USA). The Microsoft Excel macro established by the Duke Central Reference Laboratory, available at the Los Alamos National Laboratory HIV immunology database (http://www.hiv.lanl.gov/) was used to calculate the $TCID_{50}$ for each virus.

2.5.3.3 Neutralization assay

Viral inhibition activity of $IBLZ_{Fab}$ was assessed by the reduction in tat-inducible luciferase activity after a single round infectivity assay as described previously [90]. A three-fold dilution series of the total fraction of $IBLZ_{Fab}$ before SEC separation was prepared in a 96-well tissue culture plate and incubated with 200 $TCID_{50}$ of HIV-1 pseudovirus particles in a final volume of 150 µl of complete DMEM for 1 hour at 37°C. Densitometric analysis of the total sample of $IBLZ_{Fab}$ was performed in order to ascertain the amount of correctly assembled, functional Fab fragment in the total fraction (QuantityOne version 4.6.9 software). Samples of the total fraction of $IBLZ_{Fab}$ were assayed in duplicate and virus and non-virus containing wells were included as controls. Thereafter, 1 x 10^4 freshly trypsinized TZM-bl cells prepared in complete DMEM and supplemented with DEAE Dextran (20 µg/ml) at a final volume of 100 µl, were added to each well. Plates were then incubated for a further 48 hours before the luminescence was measured as described above. Each inhibition assay was performed in duplicate and for each assay triplicates were obtained for each data point, mean and standard deviation was then calculated using Microsoft Excel (Windows 7). The value to achieve 50 % inhibition (IC_{50}) was calculated by fitting a variable-slope, non-linear regression curve using GraphPad Prism version 5.00 for Windows (GraphPad Software, US).

3 Chapter 3: Results

3.1 Generation of recombinant Bicistronic IBLZ$_{Fab}$-expression vectors

A bicistronic IBLZ$_{Fab}$ expression vector was designed in order to produce and purify the Fab fragment of an anti-HIV antibody, Ibalizumab, in a bacterial expression system. The recombinant cassette contained both the heavy and light chains of the Ibalizumab Fab region. The codon optimized cassette also contained an ompA (outer-membrane protein A) leader sequence which allowed the expressed protein to be transported to the periplasm where the oxidizing environment would support correct folding and assembly of the two chains.

The IBLZ$_{Fab}$-encoding DNA was excised from the kanamycin resistant plasmid pMK-RQ (GeneArt, Germany) and this DNA was then sub-cloned into the multiple cloning site (MCS) of the digested ampicillin resistant plasmid vector, pET15b at a 1:1 molar ratio of insert DNA: vector DNA. Successful ligation of vector and insert was confirmed by restriction digestion analysis and sequencing of the recombinant expression vector. Recombinant plasmids were isolated from cultured DH5α cells and subjected to digestion with *Bam*HI and *Bgl*II. Figure 6 shows that the IBLZ$_{Fab}$ insert was excised from the pET15b expression plasmid using both restriction enzymes which resulted in a 1547 bp DNA fragment confirming the presence of the insert in the plasmid vector. Thereafter, expression plasmids containing the correct IBLZ$_{Fab}$ insert size were sequenced, verifying the correct orientation of the sub-cloned constructs (See Appendix 3).

3.2 Expression and purification of IBLZ$_{Fab}$

Recombinant IBLZ$_{Fab}$ was generated by inoculating 8 litres of LB media with transformed BL21 Star^{TM} (DE3) *E. coli* cells containing the IBLZ$_{Fab}$-pET15b expression vector. The periplasmic fraction of the bacterial cells was extracted before being purified by affinity chromatography.

Periplasmic fractions containing $IBLZ_{Fab}$ were extracted using a modified osmotic shock procedure previously described [91, 92]. This method involved re-suspending the cell pellet in an extraction buffer comprising 200 mM Tris/HCl, 1 mM EDTA, 20 % w/v sucrose and 0.5 mg mL lysozyme. *E. coli* transformed with empty pET15b vector was used as a negative control and separated alongside $IBLZ_{Fab}$ samples throughout the expression and purification procedure. Due to the impurity of the kappa matrix eluate, a second round of purification was applied in order to separate the unwanted bacterial proteins from the $IBLZ_{Fab}$ fragments. A high resolution Sephadex G-75 column was used for SEC separation of the $IBLZ_{Fab}$.

Despite the presence of the 6x histidine tag on the N-terminus of the Fab fragment, the expressed protein could not be detected on a western blot using an anti-his probe (See Appendix 3).
Regardless of this, efforts to purify the $IBLZ_{Fab}$ using Nickel affinity chromatography were attempted but proved to be unsuccessful. This may be attributed to the his-tag being incorporated into the tertiary structure of the $IBLZ_{Fab}$ fragment. Another reason that may be considered is that any post-translational modification to the target protein may have removed the his-tag, the $IBLZ_{Fab}$ protein had been transported to the periplasm as a result of the signal peptide incorporated into the construct. Accordingly, purification of the Fab fragment was achieved using a human kappa light chain specific matrix, which associated with the light chain in the variable region of the Fab fragment. Analyses of the cell lysates at different steps in the expression and purification process revealed that some protein remained in the cytoplasmic fraction of the cell. The $IBLZ_{Fab}$ fragments were expressed at very low concentrations (200 µg/ml of $IBLZ_{Fab}$ per 8 liters of culture media) and proved difficult to isolate.

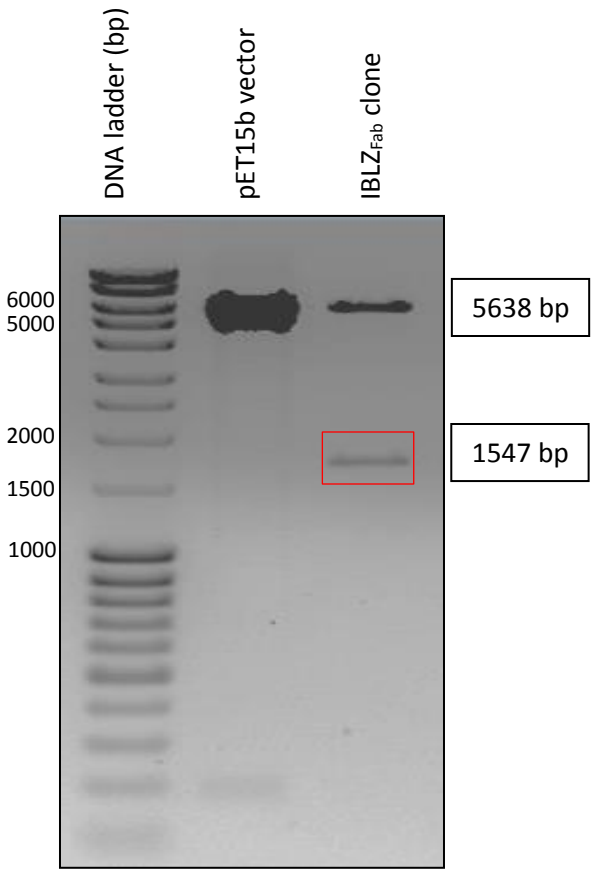

Figure 6. Restriction digestion analysis of the pET15b IBLZ$_{Fab}$ expression vector:

All DNA samples were resolved on a 1 % agarose gel, and visualized under UV light. Positive colonies selected from agar plates containing ligation reaction transformed *E. coli* were cultured overnight in LB broth and the recombinant plasmids were isolated. The plasmid DNA was then subjected to digestion analysis which resulted in DNA fragments of distinct sizes. The IBLZ$_{Fab}$ insert was excised and a DNA fragment size 1547 bp was obtained (boxed in red).

Various periplasmic extractions were attempted since western blot analysis showed a large amount of expressed $IBLZ_{Fab}$ retention in the cytoplasmic fraction of the cell lysates. Protein yield was increased by treatment on ice as well as treatment with ice cold dH_2O. Samples of total cell lysate and periplasmic fractions were analyzed by reducing and non-reducing SDS-PAGE and western blot. The negative control used in western blot analyses of $IBLZ_{Fab}$ expression and purification was *E. coli* transformed with empty plasmid vector pET15b, deficient of a protein encoding insert.

SDS-PAGE Coomassie stains were inconclusive therefore western blot analysis was performed. The Fab fragment existed in two forms; assembled Fab fragments observed at a molecular weight of ~50 kDa (heterodimers) and unassembled monomers with a size of ~25 kDa. The negative control used in all experiments illustrated banding patterns that were similar to that of the recombinant $IBLZ_{Fab}$-encoding pET15b plasmid (See Appendix 3). However western blot analysis showed a distinct difference in purified eluents (Figure 7). Despite the non-specific binding of the anti-kappa light chain antibody, western blot analysis shows the presence of the Fab fragment in the $IBLZ_{Fab}$ periplasmic fraction and eluent, at ~50 kDa, under non-reducing conditions, with no detection in the negative control (Figure 7).

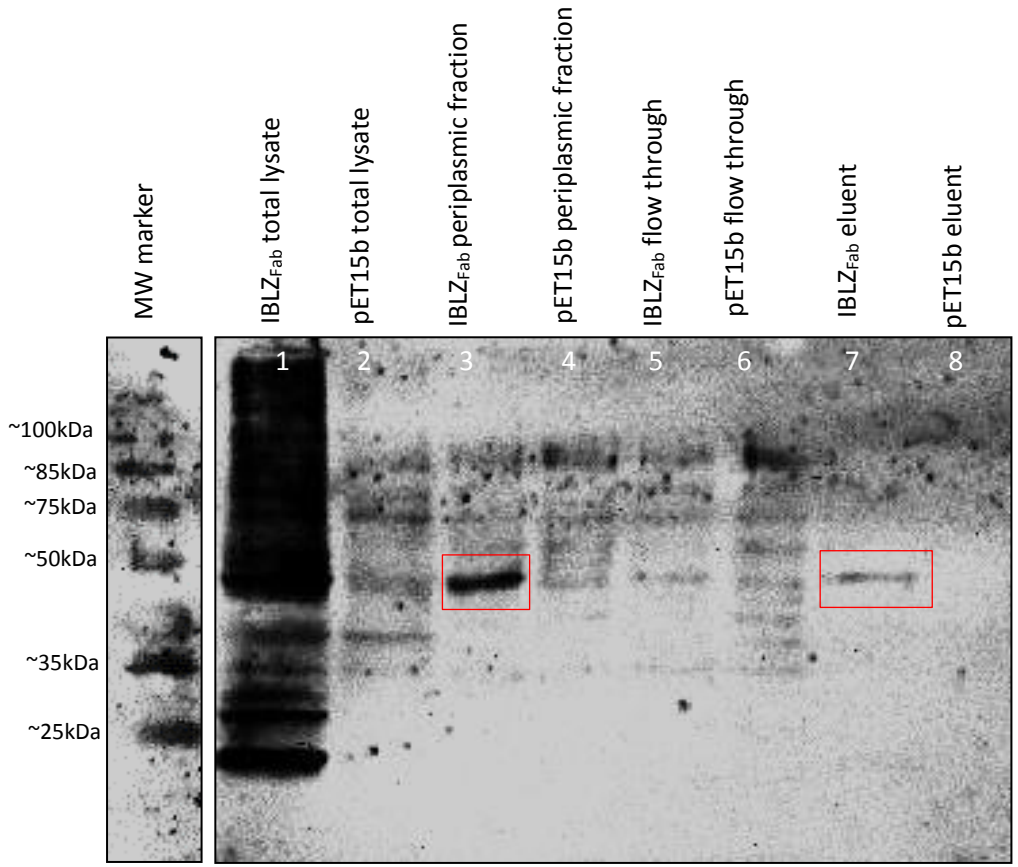

Figure 7. Western blot analysis of $IBLZ_{Fab}$ expression and purification under non-reducing conditions:

$IBLZ_{Fab}$ was detected using a human kappa light chain specific antibody (diluted 1:500). The antibody associated with the human kappa light chain on the variable region of the Fab fragment. A non-recombinant pET15b, was analyzed alongside the fragments as a negative control. Western blot detection under non-reducing conditions shows $IBLZ_{Fab}$ in the periplasmic fraction and eluent. All sample concentrations were normalized before analysis.

3.2.1 Size exclusion chromatography

In order to increase the homogeneity of the affinity purified $IBLZ_{Fab}$, the total fraction was subjected to size exclusion chromatography (SEC). The total $IBLZ_{Fab}$ fraction was applied to a Sephadex G-75 AKTA-FPLC P-920 column. Fractions contained in the same protein peak were pooled and analyzed. The separation resulted in three main fractions of interest; pooled fractions 1, 2 and 3 as well as the ~10 kDa contaminating bacterial protein (Figure 8 A). $IBLZ_{Fab}$ molecular weights represented by the peaks were determined based on the Gel filtration Low Molecular Weight (LMW) calibration kit (GE Healthcare; UK) which was applied to the column, before the total fraction of $IBLZ_{Fab}$ was separated, to illustrate where peaks of specific sizes would be eluted (Appendix 3). F1 and F2, seen in Figure 8 A, was not active despite being tested by ELISA analysis and correspond to the void volume based on the calibration curve. The Ibalizumab Fab fragments, in pooled fraction 1, correspond to a predicted size of ~50 kDa. Fractions were resolved using non-reducing 12.5 % SDS-PAGE to determine which fraction contained the Fab fragment (Figure 8 B). Western blot analysis of these fractions seen in figure 8 C confirms the presence of the $IBLZ_{Fab}$ fragment in fraction 1. Pooled fraction 1 appeared to contain the highest amount of Fab fragment detected by the anti-kappa light chain specific antibody, followed by fraction 2. The monomeric or unassembled chains are visible in pooled fraction 3. The negative control resolved alongside the fractions of interest is a 10 kDa bacterial protein, present within the total fraction of $IBLZ_{Fab}$, which has been consistently expressed. This protein was not detected using a kappa light chain specific antibody and was therefore used as a negative control. Subsequent to SEC separation ~200 µl at a concentration of ~200 µg/ml of functional, assembled $IBLZ_{Fab}$ could be isolated.

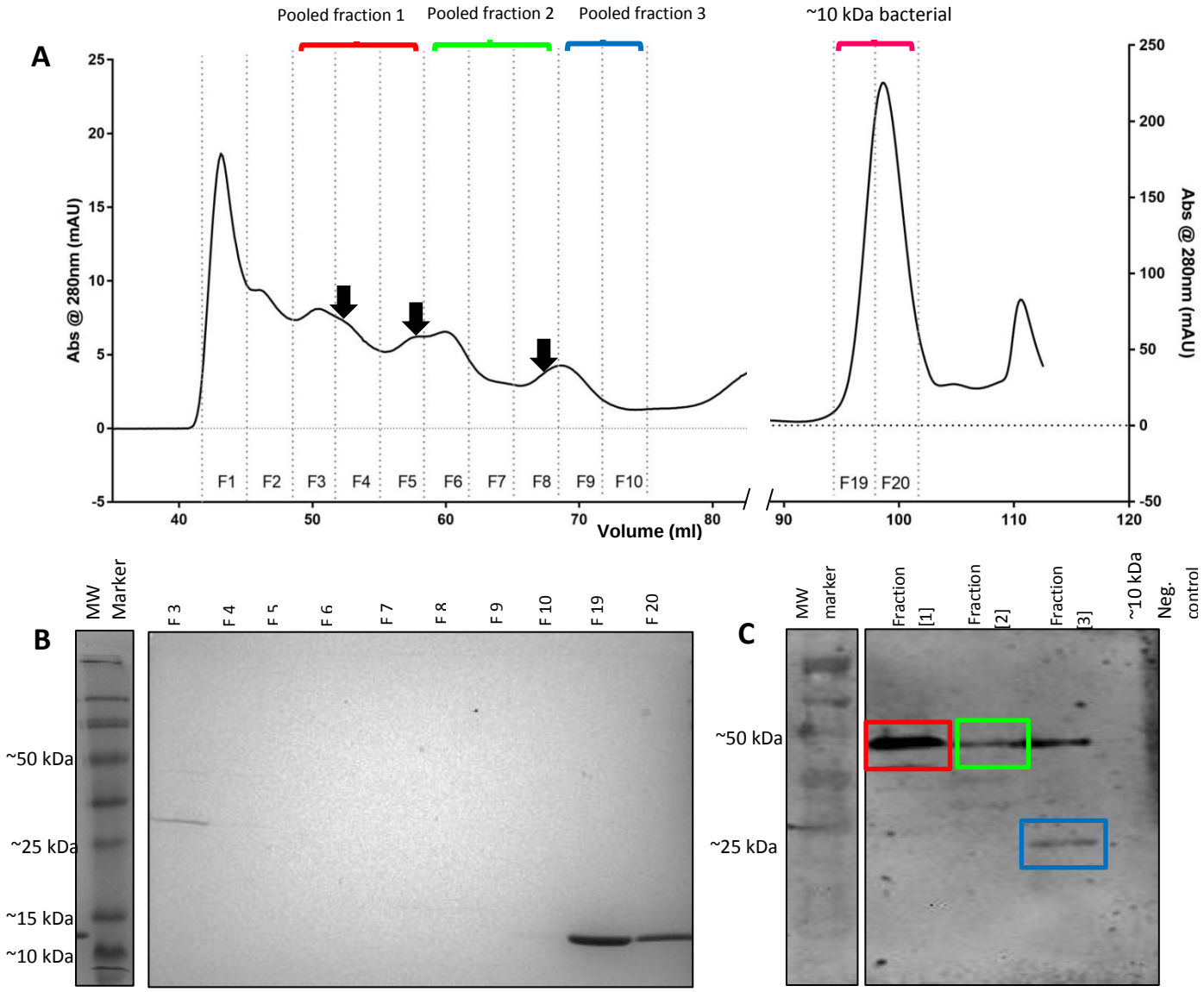

Figure 8. Elution profile of SEC separation on a Sephadex G-75 column, SDS-PAGE and western blot analysis of IBLZ$_{Fab}$

Figure **8 A** illustrates the elution profile of the IBLZ$_{Fab}$. Pooled fraction 1 (indicated by red bracket), pooled fraction 2 (green bracket) and pooled fraction 3 (blue bracket) correspond to molecular weight sizes of ~50 kDa, ~50/25 kDa and ~25 kDa respectively. This is based on LMW standards seen in appendix 3, maximum elution volumes of conalbumin, ovalbumin and carbonic anhydrous are indicated by black arrows on the figure. Fractions were collected at 3 ml intervals, those constituting one peak were pooled and concentrated. Figure **8 B** is a non-reducing SDS-PAGE analysis of SEC separated fraction (F3 to F10 and F19-F20). Fab fragments are visible in F3 and F4, and the bacterially expressed ~10 kDa is seen in F19 and F20. These fractions correspond to the elution profile in Figure 8 A. Figure **8 C** is the western blot detection of SEC separated IBLZ$_{Fab}$ fragments using anti-kappa light chain specific antibody (diluted 1:500) confirms the presence of the IBLZ$_{Fab}$ fragment in fraction 1 and 2 and the monomeric or unassembled chains in fraction 3. The bacterially expressed ~10 kDa protein is not detected by a kappa light chain specific antibody.

3.3 Functionality testing of $IBLZ_{Fab}$

The integrity and binding capacity of $IBLZ_{Fab}$ was tested using ELISA and SPR analysis. The viral inhibition efficacy of the Fab fragment was also tested using viral neutralization studies.

3.3.1 Enzyme-linked Immunosorbent Assay (ELISA) Analysis of $IBLZ_{Fab}$

Three main ELISA formats were used. The first ELISA involved binding the total, affinity purified fraction of $IBLZ_{Fab}$ to 2dCD4 in order to determine whether the Fab fragment associated correctly with 2dCD4. The highest signal was observed at the highest concentration and the weakest at the lowest concentration of the total fraction of $IBLZ_{Fab}$. For improved separation of $IBLZ_{Fab}$, a Sephadex G-75 column was used. The SDS-PAGE analysis of these fractions indicated that the 50 kDa Fab fragment was most likely in pooled fraction 2 (See Appendix 3). However, ELISA analysis showed that the most active fraction with the highest concentration of functional Fab fragment was pooled fraction 1 (Figure 9), concentration was determined by means of the BCA assay (see Appendix 1). The binding by pooled fraction 1 is vastly greater than that of the total fraction before SEC separation.

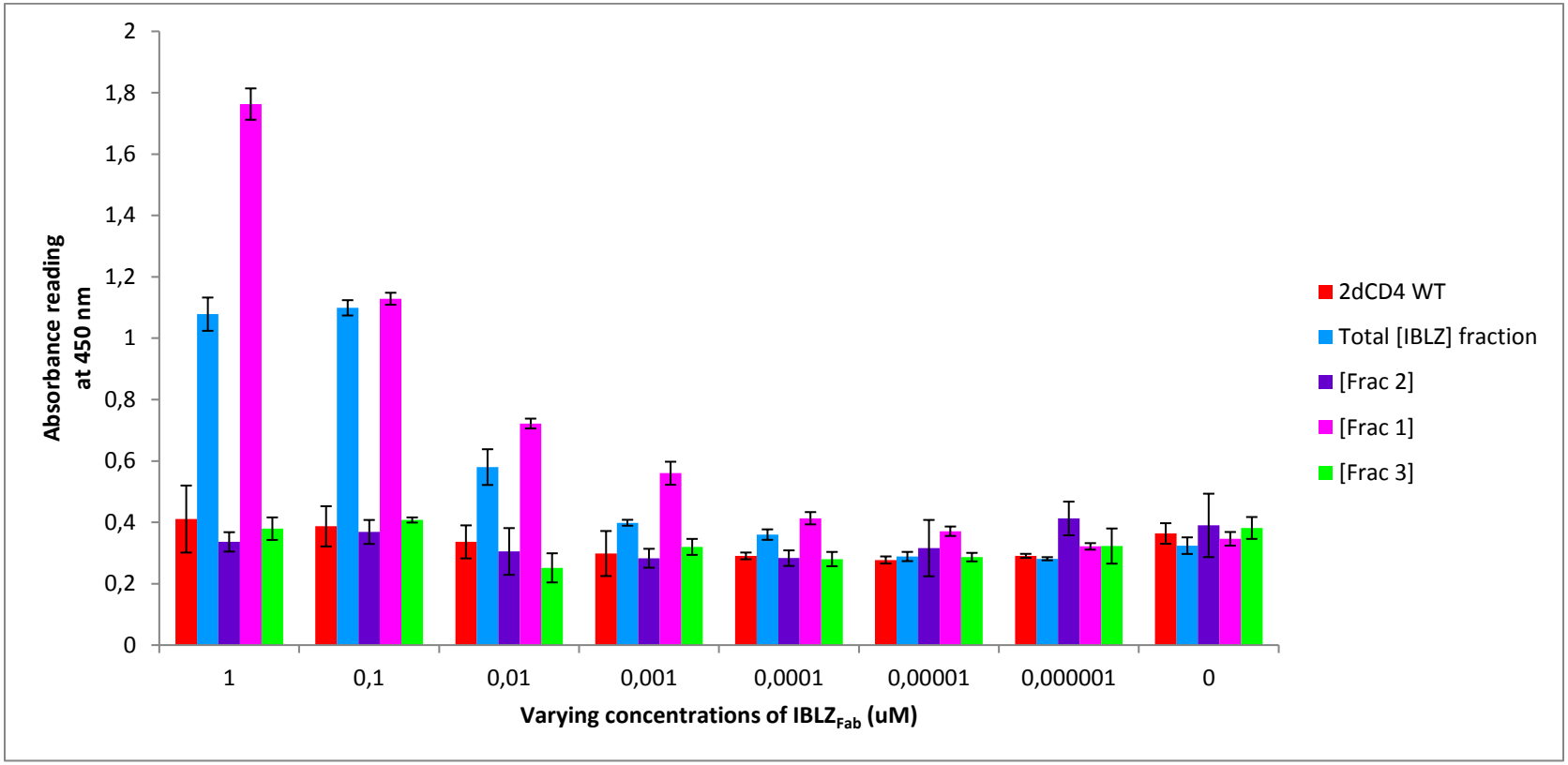

Figure 9. Detection of $IBLZ_{Fab}$ bound 2dCD4:

The 2dCD4-$IBLZ_{Fab}$ complex was detected with an anti-kappa antibody. Each experiment was performed in triplicate to obtain an average absorbance, standard deviation was also calculated (refer to error bars within the figure). Fraction 1, seen in pink has the highest signal at the highest concentration compared to the other fractions, indicating it is the most active fraction. Fraction 2 in purple and fraction 3 in green are not as active as predicted. However, the SEC separated fractions show an increased association compared to the total $IBLZ_{Fab}$ fraction (blue) before separation.

Ibalizumab is non-immunosuppressive and does not hinder the binding of viral gp120 proteins to CD4. In order to test the functionality of this microbially expressed $IBLZ_{Fab}$ an ELISA was performed to detect the binding of gp120 to WT 2dCD4 in the presence of $IBLZ_{Fab}$. Figure 10 shows that the microbially expressed $IBLZ_{Fab}$ does not prevent gp120 from binding to 2dCD4. The interaction between gp120 and CD4 was confirmed by the signal produced by 2G12, a monoclonal antibody that recognizes a distinct neutralization epitope on the gp120 glycoprotein of HIV-1 [93]. The 2G12 epitope is mannose dependent and is located on the high-mannose glycans of residues 295, 332, and 392, with peripheral glycans from residues 386 and 448 on either side [94]. This epitope is believed to have no direct contact with the gp120 polypeptide surface.

A strong signal is also produced when detecting with 17b (Figure 10), an antibody that binds the CD4-induced form of gp120 (CD4i). The absorbance signal produced when detecting with 17b was observed in the 2dCD4-gp120 complex in the presence and absence (negative control) of the $IBLZ_{Fab}$ fragment. The CD4i form of gp120 facilitates co-receptor binding; inhibition by Ibalizumab does not prevent this interaction. The structural integrity within domain 1 and domain 2 of CD4 is not essential for HIV-1 entry or inhibition by Ibalizumab. Freeman *et. al.* [75] showed that it is therefore unlikely that Ibalizumab would directly block gp120 binding to the co-receptor on the cell surface. It is believed that the binding of Ibalizumab affects downstream conformational changes that ultimately prevent viral entry into the host cell [75].

The results seen in Figure 10 support the objective of this study, affirming the fact that the protein which has been successfully expressed and purified in a bacterial expression system does not impair the binding of gp120 to 2dCD4 and does indeed bind to 2dCD4 in the presence of gp120. Based on sequence analysis of the construct this protein corresponds to the Fab fragment of Ibalizumab (Appendix 2). It can be concluded that this protein associates with CD4 at an epitope away from the binding site of gp120 and MHC class II molecules.

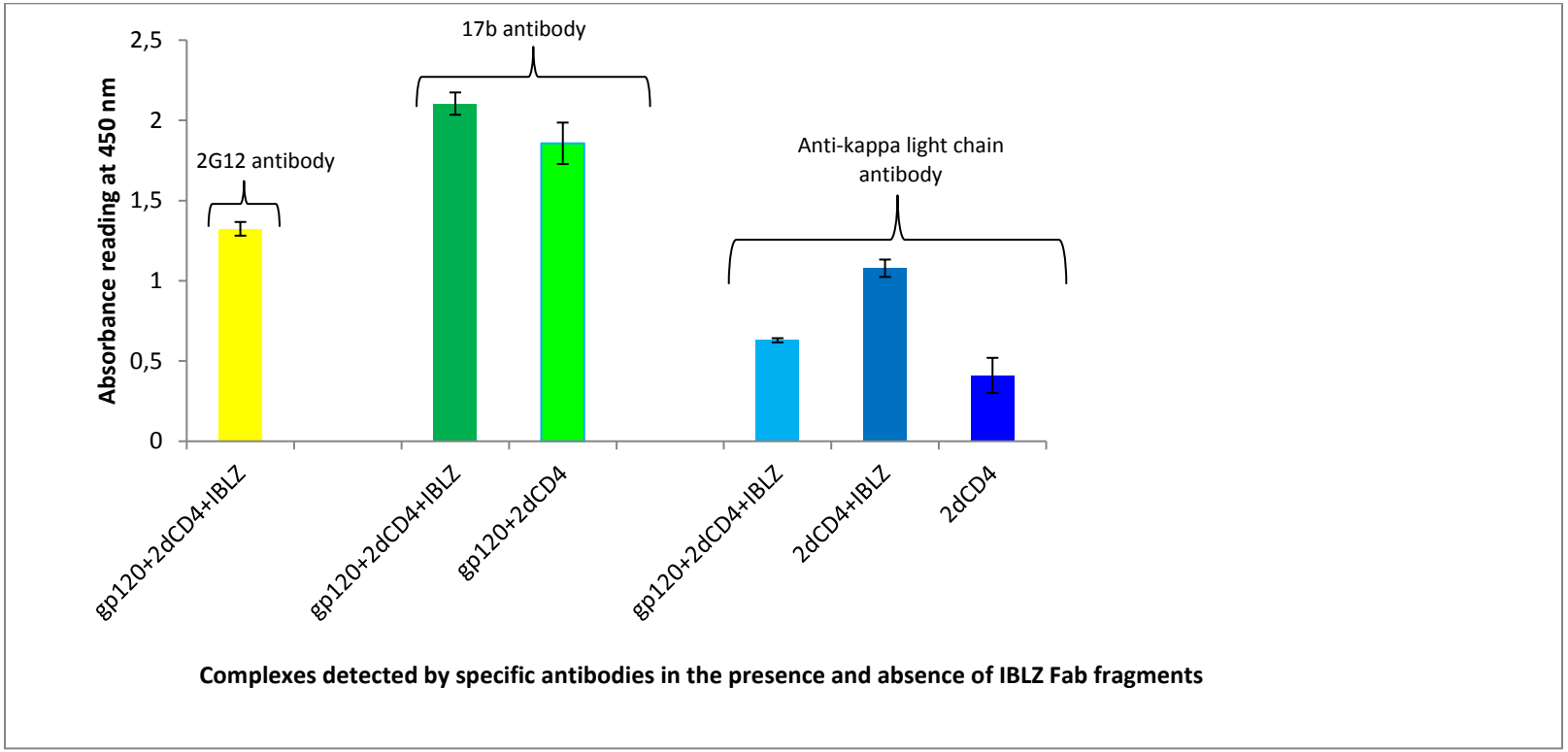

Figure 10. Detection of the interaction between WT 2dCD4 and gp120-BAL in the presence of $IBLZ_{Fab}$:

The interaction of gp120 and 2dCD4 in complex with $IBLZ_{Fab}$ was detected using a gp120 specific antibody, 2G12 (yellow) and a gp120 CD4 induced site specific antibody, 17b (green). Each experiment was performed in triplicate to obtain an average absorbance, standard deviation was also calculated (refer to error bars within the figure). The signal seen in blue is that of the kappa light chain specific antibody, illustrating the presence of the Ibalizumab Fab fragment in the complex, this decreased signal may be due to the presence of gp120 in the complex. Controls deficient of the fab fragment were analyzed alongside the experiment (signals seen in light green and dark blue).

3.3.2 Surface Plasmon Resonance (SPR) Analysis of $IBLZ_{Fab}$

The kinetics of the $IBLZ_{Fab}$-2dCD4 interaction was tested using SPR. The fraction with the highest 2dCD4 binding activity, fraction 1, as measured using ELISA was used in SPR studies. Purified 2dCD4-WT was immobilized on a GLC sensor chip. Total fraction concentration was used to prepare samples from 250 nM to 0 nM. Due to the contamination seen in the SDS-PAGE analysis (See Appendix 3), densitometry could not be performed on the sample. The association rate (k_a), dissociation rate (k_d), and equilibrium dissociation (K_D) constants for the reaction between 2dCD4 and $IBLZ_{Fab}$ were calculated by fitting the resultant sensograms directly to a 1:1 Langmuir binding model using the ProteON Manager software. The calculated affinity for the interaction between 2dCD4-WT and $IBLZ_{Fab}$ was 11.3 nM, similar to K_D values published by others [95] (Figure 11).

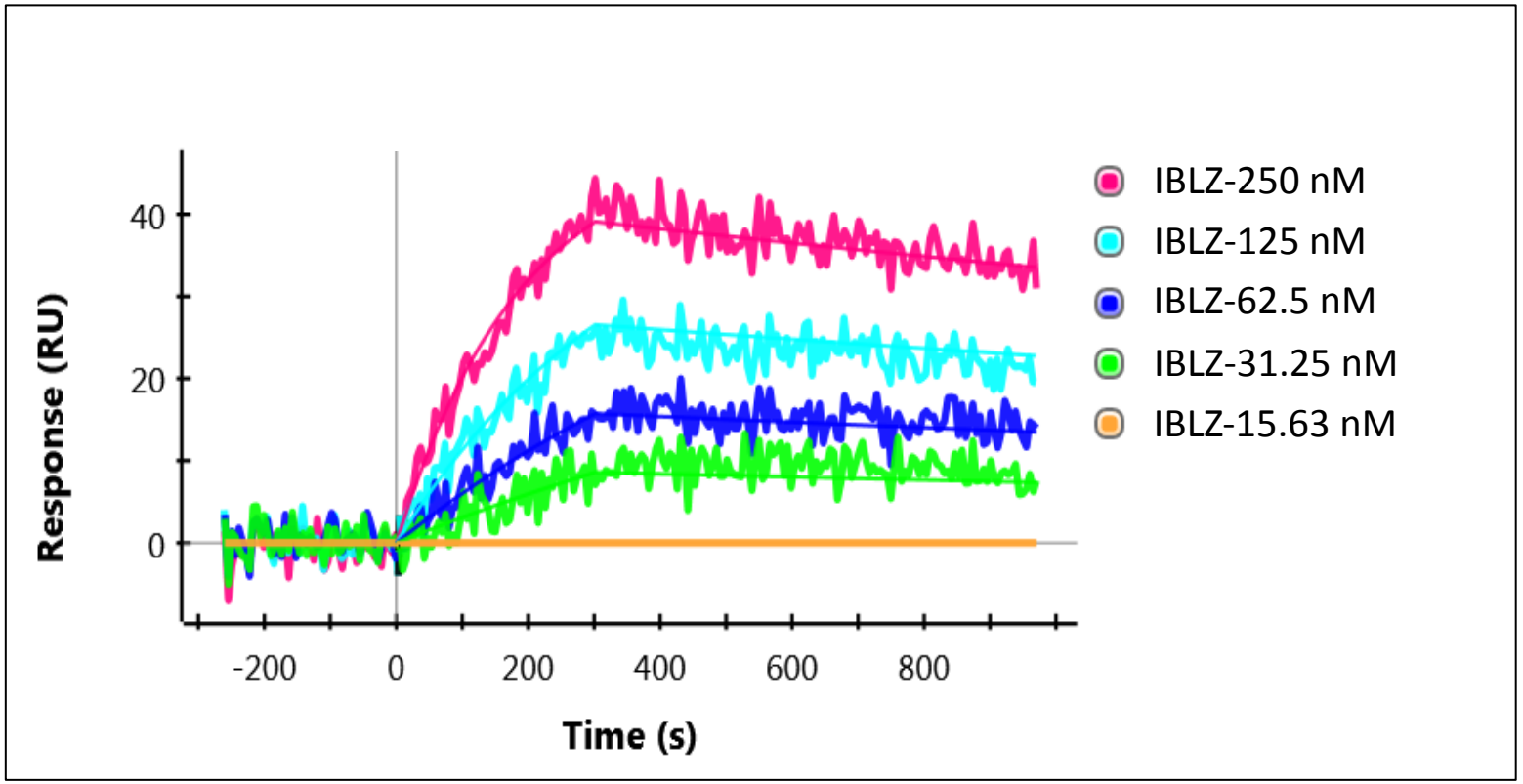

Figure 11. 2dCD4-IBLZ$_{Fab}$ interaction analysis by SPR:

Microbially expressed IBLZ$_{Fab}$ at concentrations ranging from 250 nM down to 0 nM were passed over immobilized 2dCD4 (0.1 mg/ml) at a flow rate of 5 µl/min for 5 minutes. A K_D value of 11.3 nM was calculated, with an association constant (k_a) of 2.02 x 10^4 Ms^{-1} and a dissociation constant (k_d) of 2.29 x 10^{-4} s^{-1}.

3.3.3 Viral inhibition: Neutralization Assays of $IBLZ_{Fab}$

In order to test the inhibiting properties of the microbially expressed $IBLZ_{Fab}$ *in vitro,* in house neutralization assays were performed using two pseudoviruses; CAP210 and SF162. The total fraction $IBLZ_{Fab}$ was used in the neutralization assays since obtaining a satisfactory concentration of the pure $IBLZ_{Fab}$ proved challenging.

The total fraction of $IBLZ_{Fab}$ was used at final concentration of 125 µg to account for the contaminating proteins present in the preparation. Based on the densitometric analysis of the SDS-PAGE non-reducing coomassie gel, of the total fraction, approximately 13.97 % appeared to be correctly assembled $IBLZ_{Fab}$ (Figure 12). Since only the 10 kDa protein eluted with the Fab fragment using the anti-kappa specific matrix and did not exhibit any activity in ELISA analyses, it was used as a negative control in order to confirm that any inhibition seen in the assays were indeed from $IBLZ_{Fab.}$ The 10 kDa protein was extracted and co-purified with the total fraction of $IBLZ_{Fab.}$ A pure sample of this protein was then obtained through SEC separation of the total fraction of the fab fragment (Figure 8).

Enfuvirtide or T_{20} is a fusion inhibitor, which disrupts the formation of the 6HB thereby preventing virus entry into the host cell. T_{20} was used as a positive control to ensure the assay was functional (Figure 13 A). In addition, $IBLZ_{Fab}$ was able to neutralize approximately 50 % of pseudovirus CAP210 and ~20 % of pseudovirus SF162 (Figure 13 B). No inhibition was detected with the ~10 kDa negative control, attributing all neutralization activity to active $IBLZ_{Fab}$ fragment. VSV-G was used as a negative control, in order to confirm specificity for HIV-1 neutralization (Figure 13 C).

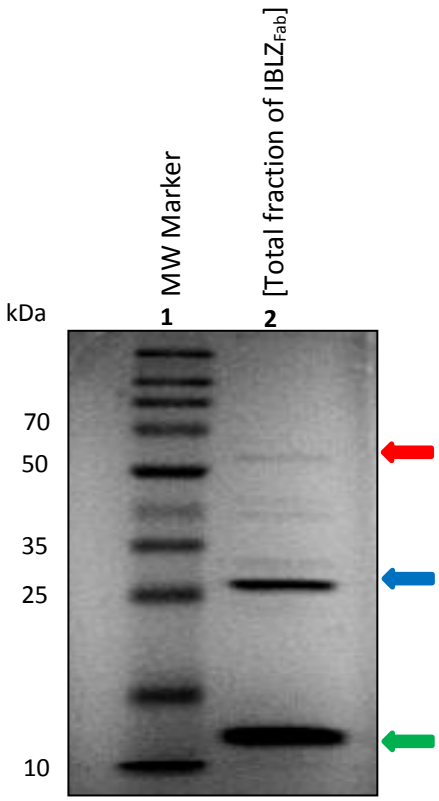

Figure 12. Non-reducing SDS-PAGE Analysis of 3 µg of total fraction of $IBLZ_{Fab}$:

The total fraction of $IBLZ_{Fab}$ (3 µg) was separated under non-reducing conditions, this image depicts the Fab fragment at 50 kDa (indicated by the red arrow), unassembled chains at 25 kDa (indicated by the blue arrow) and a 10 kDa contaminating protein (indicated by the green arrow). The co-purified 10 kDa protein was used as the negative control in neutralization assays. According to densitometric analysis approximately 13.97 % appeared to be correctly assembled $IBLZ_{Fab}$.

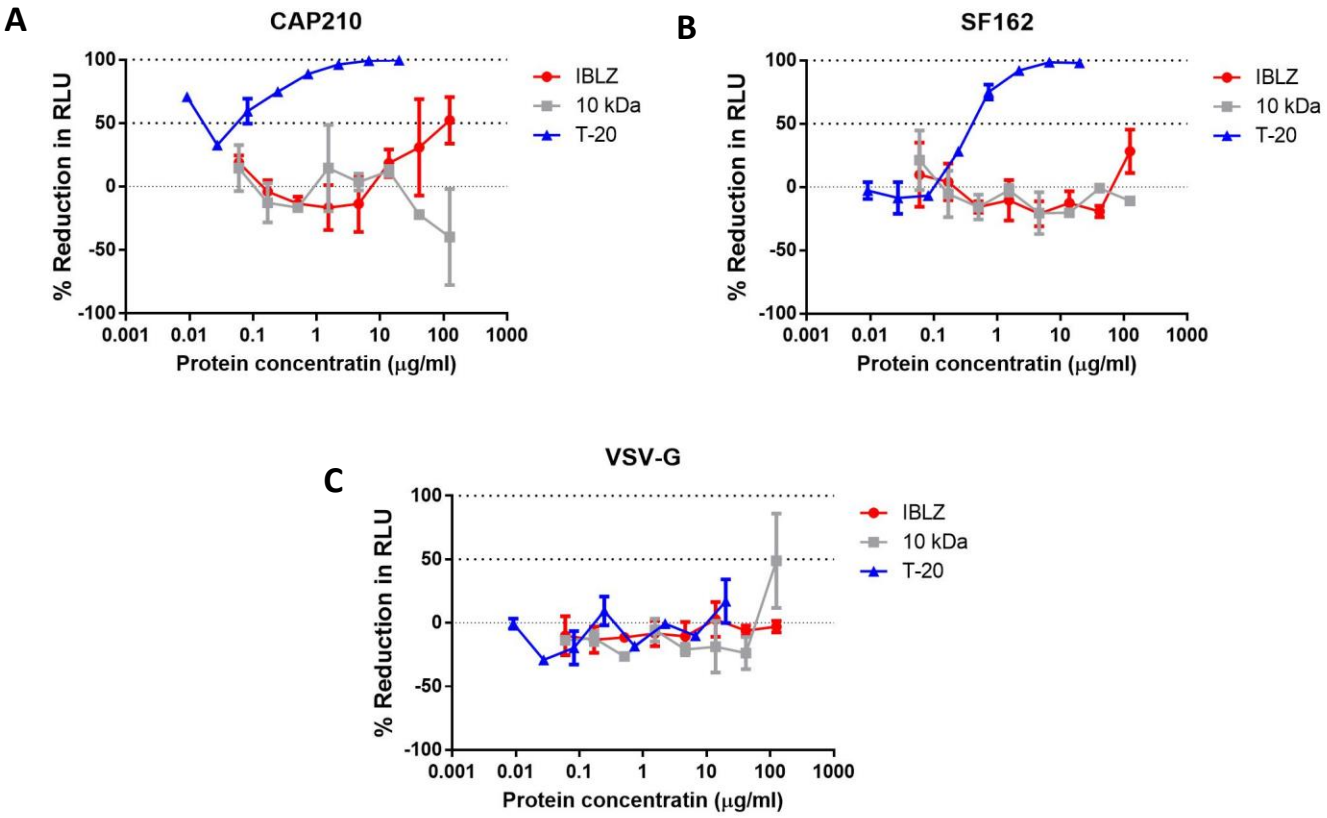

Figure 13. Neutralization Assay of pseudoviruses CAP210, SF162 and VSV-G against entry inhibitor Enfuvirtide (T_{20}) and $IBLZ_{Fab}$:

T_{20} was used as a positive control and tested alongside each pseudovirus challenged with $IBLZ_{Fab}$; reproducibility of the control in each assay was successful. Graph **13 A** illustrates the average viral percent inhibition of CAP210 by entry inhibitor T_{20} and $IBLZ_{Fab}$ (seen in blue and red, respectively), 100 % inhibition with T_{20} was achieved at 20 µg/ml, the highest concentration of T_{20}. An acceptable IC_{50} value of approximately 0.36 µg/ml was obtained. Neutralization of CAP210 by $IBLZ_{Fab}$ achieved 50 % viral inhibition (seen in red) at the highest concentration of the total fraction of $IBLZ_{Fab}$, 125 µg/ml. The 10 kDa protein used as a negative control showed no activity (seen in grey) or inhibition. Graph **13 B** illustrates the average viral percent inhibition of SF162 by IBLZ and T_{20}. Neutralization of $IBLZ_{Fab}$ against SF162 achieved ~20 % viral inhibition seen in red. T_{20} obtained 100 % inhibition (visible in blue). Graph **13 C** depicts the negative control of VSV-G run alongside all neutralization assays, no neutralization was observed by the IBLZ fraction (in red), confirming neutralization data obtained from the assay is attributed to the active fraction containing functional $IBLZ_{Fab}$ fragments.

4 Chapter 4: Discussion and Concluding remarks

Ibalizumab is a humanized anti-CD4 monoclonal antibody with potent HIV-1 inhibitory effects and has been FDA approved as an anti-HIV-1 therapeutic agent [96]. This study investigated the feasibility of expressing a functional Ibalizumab Fab fragment using a microbial expression vector.

Despite the relatively high production costs of mammalian antibody production, approximately 95 % of all currently available therapeutic antibodies are still produced in mammalian cell culture systems [85]. Folding, secretion and post-translational modification observed in mammalian expression systems produce antibodies which are comparable to those produced by the human body [85]. In the case of commercially available antibodies as therapeutic agents, production requires a significant increase in yield. For instance, in some high-dose antibody therapies that require more than 200 kg of purified product, the costs may exceed $500/g of protein per annum supposing a productivity of 2 g/L with a 50 % process yield [44].

Bacterial expression systems are unquestionably more cost effective and allow expression of antibody fragments such as Fab and scFV fragments [44]. In contrast to the cost of mammalian protein expression, bacterial cell culture and purification reagents cost around $1000 for approximately 50 liters of cell culture media. As an example, the commercially available digoxin Fab fragment, DigiFab, used for the treatment of digoxin intoxication is expressed in Gram negative *E. coli* cells [97] much like this study. Over expression of the Digoxin fab fragment is temperature induced, and a protein yield of 0.8 mg/L is achieved through the shake flask expression system [85]. Not all Fab fragments, such as $IBLZ_{Fab}$, are able to express under the same conditions and require independent optimization. *E. coli* has always been the favored expression system for recombinant protein production, which can be attributed to the many advantages this

system offers apart from being cost effective. These include high growth rate, simple cell media requirements, ease of handling and high yield [98].

Bacterial cells are not an ideal expression system for the production of antibodies as these are complex polyproteins [99]. However, bacterial expression of certain antibody fragments can be achieved by export of the heavy and light chains to the periplasm for correct folding and formation of disulfide bonds [99]. Signal peptides in *E. coli* are used to transport pre-proteins from their point of synthesis to their final localization through various secretory pathways [92]. One such signal that has been employed in bacterial protein expression is the ompA signal sequence. The unfolded translated heavy and light chains, in the cytoplasm, are targeted by the N-terminal ompA secretion signal which directs the polypeptides to the periplasm via the secretory-dependent transport pathway [100]. Upon secretion to the periplasm the ompA signal sequence is cleaved by resident peptidases and the Fab fragment chains are allowed to assemble [101]. In the periplasm, disulfide oxidoreductases and isomerases catalyze the formation of disulfide bonds between the heavy and light chains, enabling the accumulation of correctly folded, soluble Fab fragments [102]. Therefore, successful bacterial expression of an effective anti-HIV monoclonal antibody such as Ibalizumab will have a significant impact on antibody therapeutic approaches in countries like South Africa.

One approach that may be employed for the bacterial production of the Ibalizumab fab fragment in *E. coli* is the independent expression of the heavy and light chain; $IBLZ_H$ and $IBLZ_L$. Individual expression vectors may be designed, consisting of either the $IBLZ_H$ chain or the $IBLZ_L$ chain. Expressed chains may then be extracted from harvested bacterial cells and purified using a well-established affinity chromatography procedure. Following affinity purification of $IBLZ_H$ and $IBLZ_L$, a reconstituted fab fragment may be generated by optimized oxidative refolding procedures. An alternative approach that was applied in this study, is the bicistronic expression of the $IBLZ_{Fab}$. This involved co-expression of the $IBLZ_{VH,}$ $IBLZ_{CH1}$ and $IBLZ_{VL,}$ $IBLZ_{CL}$ on a single plasmid which allowed *in vivo* reconstitution in the presence of protein folding enzymes in the periplasmic environment. This approach has been documented to be more efficient than *in vitro*

reconstitution, and potentially improved the quality of the recombinant protein despite the poor yield [103]. The banding patterns on the SDS-PAGE gels of the periplasmic fractions, shown in appendix 3, are typical for antibody expression in *E. coli* documented in the literature [43, 91, 99, 104].

According to some of the literature [43, 44, 85, 91] the best approaches to expressing functional antibody fragments in bacteria take advantage of its secretory system. This process, first described in 1988 [105], allows correct folding of the Fab fragment by exporting the translated light and heavy chains of the Fab to the oxidative environment of the periplasm resulting in the correctly folded heterodimer Fab. Fab fragments that are secreted to the periplasm for correct folding usually result in low yields, but expression in the reducing environment of the cytoplasm results in non-functional or unfolded protein chains [106].

Optimal protein expression of the Ibalizumab Fab fragment was achieved in the absence of isopropyl-1-thio-β-D-galactopyranoside (IPTG). IPTG serves as a mimic of the naturally occurring allolactose that is an inducer of the *lac* operon. IPTG is often used at final concentrations ranging from 0.5-1.0 mM. Reports on induction strategies show highest Fab yields were obtained by induction with low IPTG concentration [107]. However, over expression of the Fab fragment, with the bacterial expression methods applied in this study, remained consistent in the presence and absence of IPTG. This was due to 'leaky' transcription initiated by the T7 promoter in the plasmid vector. Therefore, induction of the over expression of the Ibalizumab Fab fragment in this study occurred in the absence of IPTG.

Non-specific bacterial proteins co-purified with the assembled and unassembled Fab fragments. The co-purification of these bacterial proteins could be attributed to unoccupied binding sites on the kappa matrix resin. The large amounts of periplasmic extraction lysate required for obtaining an acceptable amount of the low yield fab fragment and poor binding efficiency of the Fab

fragment, may have contributed to the non-specific binding of these bacterial proteins to the matrix.

The elution profile (seen in Figure 8) of $IBLZ_{Fab}$ indicates the absorbance (mAU) of the heterodimeric form of the protein at ~8 mAU, consistent with the findings of others [81]. The aforementioned study, conducted by Pace, *et. al.* created Ibalizumab based bi-specific broadly neutralizing antibodies (biNAbs) by fusing the scFv of PG9 and/or PG16 to the N-terminus of the heavy chain of Ibalizumab [81]. The biNAbs were expressed in 293A cells and SEC separation was applied in order to obtain the functional, heterodimeric antibody (~50 kDa) from the cell lysate. The elution profile of the biNAbs including unconjugated Ibalizumab, which was used as parent control, was consistent with the findings of this study.

Low amounts of functional $IBLZ_{Fab}$ were recovered from the periplasmic fraction of the bacterial cell. The efficiency of Fab fragment production in *E. coli* varies between different cell strains and growth conditions [43]. A single protein located in the periplasm of *E. coli* (Skp) has been shown to increase the over expression of fusion proteins, [108]. Skp is a chaperone protein, believed to be involved in the transport of outer-membrane proteins, such as the ompA signal sequence [109]. Skp is expressed at varying levels in different *E. coli* strains [43]. A study led by Corisdeo *et. al*. showed that *E. coli* strains JM105 and BL21 produced the highest levels of Fab fragment recovered [43]. Therefore, the difference of Fab fragment yield may be attributed to the amount of Skp proteins produced during over expression, transport and folding of the proteins [43]. This study made use of the BL21 *E. coli* strain and ompA signal sequence, in order to increase the yield of the recombinant Ibalizumab Fab fragment.

The poor Fab fragment yield could also be related to the excess strain of the bacterial secretory system [99]. Robust expression systems are usually preferred, so as to gain maximal yield of recombinant proteins [99]. However, using these strong expression systems exerts a tremendous

metabolic stress on the host cell metabolism [110]. The use of powerful induction promoters, such as the T7 promoter used in this study, when expressing Fab fragments in *E. coli* overloads and saturates the host's secretory system [99]. This saturation of the secretory system may be one of the reasons that poor yields of the recombinant $IBLZ_{Fab}$ fragments were recovered. Even so, functionality tests were performed in order to test the binding capacity and the viral efficacy of the Fab fragment.

Functionality of the bacterially expressed $IBLZ_{Fab}$ were investigated by: (1) ELISA analysis to test the modular association of $IBLZ_{Fab}$ and 2dCD4; (2) SPR analysis to ascertain the binding kinetics of $IBLZ_{Fab}$ to 2dCD4, and (3) viral inhibition assays to evaluate the neutralization efficacy of bacterially expressed $IBLZ_{Fab.}$

The non-immunosuppressive properties of Ibalizumab make it a favourable candidate for anti-viral therapy. It has a distinct epitope from other anti-CD4 molecules by binding to the interface of D1 and D2 of CD4 away from the binding site of MHC class II molecules [17, 75, 76]. ELISA analyses were performed to test whether the Fab fragment expressed in bacteria exhibited the same binding capacity (see Figure 9). In addition to $IBLZ_{Fab}$ associating with CD4, the binding of gp120 to WT 2dCD4 in the presence of $IBLZ_{Fab}$ was also assessed (refer to Figure 10). $IBLZ_{Fab}$ should not obstruct the binding of viral gp120 proteins to CD4 [75]. Analyzing the efficiency of 17b uptake provides an additional control for the quality of the gp120-CD4 interaction in the presence of $IBLZ_{Fab.}$

The calculated affinity for the interaction between 2dCD4-WT and $IBLZ_{Fab}$ by SPR analysis was 11 nM. For the bivalent form of Ibalizumab, K_D values range from 4.3 nM to even low picomolar values. The efficiency of viral inhibition of the bivalent IgG and monovalent Fab fragments vary greatly among different viral isolates [75]. Still, both the IgG and Fab fragment of Ibalizumab can block infection [75].

The impressive CD4-binding kinetics and HIV-neutralizing properties of Ibalizumab led Pace *et. al.* to develop a bispecific bNAb (biNAb) that combines the efficacy of Ibalizumab with anti-gp120 bNAbs [81]. The study assessed the binding affinities of the biNAbs (PG9-IBLZ) as well the parent antibodies (PG9 and Ibalizumab) by SPR. The analytes used in the SPR experiment included soluble CD4 and gp120 (BaL strain) [81]. A K_D value of 15 nM, for the parent Ibalizumab antibody associated to CD4, was reported [81]. The findings of this study is consistent with data published by others [81], approving the binding affinity of the bacterially expressed recombinant $IBLZ_{Fab.}$

Two of the biNAbs designed (PG9-Ibalizumab and PG16-Ibalizumab) exhibited extraordinary breadth and potency, neutralizing 100 % of the 118 tier 2 and 3 viruses tested. The viral activity of Ibalizumab based biNAbs are the only antibody-like molecules thus far that are able to neutralize 100 % of all viruses tested at low picomolar concentrations [81]. This enhanced activity is said to be due to the mechanism of action of Ibalizumab, by associating with the ectodomain of CD4, it anchors the biNAb to the infected cell allowing viral inhibition through synergistic activity of the two molecules [81]. The viral inhibition by this biNAb, PG9-IBLZ, is said to be enhanced not only through the action of the two active agents working in concert but the longer reach of the anti-Env scFv on the fusion molecule [81]. It is believed to permit bivalent binding of more than one gp120 molecule on the surface of the virus, this results in improved antibody affinity and ultimately viral neutralization [81]. The conjugation of Ibalizumab to PG9 is also said to anchor the biNAb to CD4 at the cell surface allowing the inhibitory activity to be concentrated at the required site [81]. Obtaining binding affinity values comparable to that of the literature confirms that microbial expression of the Ibalizumab Fab fragment is not only possible but binds to CD4 with the same affinity as mammalian expressed $IBLZ_{Fab}$ fragments. This supports the main objective of this project.

Single-round *in vitro* infectivity assays were performed to provide a quantitative measure for evaluating the neutralization activity of the bacterially expressed $IBLZ_{Fab}$ fragments. Two HIV-1 Env-pseudotyped viruses, SF162 and CAP210 were chosen in order to evaluate the reproducibility of the data published by others [75].

The IC_{50} values of the Ibalizumab Fab fragment ranges between 0.02 – 0.16 μg/ml [17]. The neutralizing activity seen against SF162 was consistent with that of published data, at a concentration of >100 μg/ml pure Ibalizumab was able to neutralize ~24 % of SF162 [75]. The data obtained in this experiment cannot be directly compared to published data since a pure sample of $IBLZ_{Fab}$ fragment was not used.

The main objective of the viral inhibition studies was to evaluate whether the Fab fragment had any detectable neutralization activity. Even though neutralization activity was obtained at a high concentration the bacterially expressed $IBLZ_{Fab}$ fragment was able to inhibit viral entry.

4.1 Concluding Remarks

This study illustrates the possibility of expressing and purifying functional Ibalizimab Fab fragments using a bacterial expression system. Despite this, it does not seem feasible to produce this recombinant antibody fragment in the *E. coli* system adopted in this study, as the yield is very low and the purification processes involved are both time consuming and laborious.

E. coli is one of the most important recombinant protein expression hosts used, though antibody expression proves challenging since these organisms do not have the necessary cellular machinery to glycosylate proteins [44]. Traditionally monoclonal antibodies are produced in mammalian cell culture mostly due to functional motifs within the Fc region of the antibody, which are responsible for effector ligand recruitment [44, 111], that require the presence of an accessible carbohydrate structure at Asn^{297}. Mammalian expression systems, unlike bacterial expression systems, are equipped with the necessary cellular machinery required to generate these oligosaccharides which are analogous to those produced in the human body [44]. Mammalian cell lines are the leading expression systems for recombinant antibody production

[85]. Still, alternative production systems may be used to decrease the cost of antibody expression. Apart from bacterial expression systems, some cost effective methodologies include eukaryotic expression systems distinct from mammalian cell lines that are able to produce recombinant antibodies. These include yeast, protozoa, filamentous fungi and even transgenic plants and animals [85].

Yeast cells combine the ability of both eukaryotic as well prokaryotic expression systems with a short generation time and ease of genetic manipulation in addition to simple media requirements and stability much like microbial hosts [112]. In recent times, a multicellular parasite *Leishmania tarentolae* has been tested as an expression system for various recombinant proteins [113, 114]. Some of these include amylase, green fluorescent protein [115] and even HIV-1 gag proteins [116]. This protozoan organism has the ability to mimic mammalian glycosylation and is able to perform *N*- and *O*-glycosylation; both processes are highly conserved in mammalian cell lines [113, 117]. This system can be adapted for large up-scaling, it has easy genetic manipulation, and has minimal nutrition requirement [113]. As a result *L. tarentolae* is being explored for the production of recombinant antibodies [118].

Another area that is being explored for the expression of recombinant antibodies is transgenic plants [85]. Plants are able to perform the necessary post translational maturation required for the functional biological activity of therapeutic proteins [119]. This expression system allows cost effective up-scaling of production, though plants lack the processing machinery required for authentic *N*-glycosylation patterns which pose a challenge since enormous amounts of plant material may have to be processed [120]. Expression, folding and assembly may involve the expression of the heavy and light chains in a single plant or two individual plants [119]. Expression can be initiated by the co-transformation of separate gene cassettes or by a single expression cassette [121]. For increased expression levels or to establish a transgenic line, expression may be manipulated depending on the specific requirements of the mAb of interest [121]. In order to avoid the unbalanced expression of the heavy and light chains, careful selection of regulatory

elements such as the promoter and terminator is crucial [121]. Some successfully expressed therapeutic antibodies, vaccines and antigens in plants for infectious diseases include HIV-1 tat protein expressed in *Spinacea oleraceae [122]*, rabies peptide expressed in *Nicotiana tabacum* [123], smallpox B5 antigenic domain expressed in *Brassica oleracea* [124], hepatitis B core protein expressed in *Nicotiana tabacum* [125] and severe acute respiratory syndrome (SARS) spike protein and virus fragments also expressed in *Nicotiana tabacum* have been reported [126].

Recently, a group of researchers were able to express and purify 2G12 in transgenic tobacco plants that were subsequently accepted by the UK national pharmaceutical regulator [127]. An in-human, placebo-controlled, double blind phase I safety study of plant-derived 2G12 was then conducted, the first of its kind [127]. The antibody yield in the T1 generation was approximately 10 μg/g but increased and stabilized to ~25 μg/g in the T5 generation [127]. HIV-1 neutralizing antibodies such as 2G12 are used as immunoprophylaxis, therefore large doses of these proteins are required for effective protection [128]. In order to keep up with the global demand the production capacity is required to exceed 1000 kg/year [128]. The demand for these products are primarily in developing countries therefore costs need to be kept low, this in turn means conventional manufacturing approaches cannot be effected [127]. Plant-based engineering is consequently an attractive approach due to the low cost and scalability [127].

To date, mammalian cell lines are the most widespread expression systems for recombinant therapeutic antibodies. Other approaches that may be employed to decrease cost do not always result in the expression of a fully functional antibody but can be used in some *in vitro* applications such as research and diagnostics, where glycosylation patterns do not play a pivotal role [85]. Since Ibalizumab is a therapeutic antibody the integrity of this mAb is essential for its anti-HIV activity, correct folding and assembly of the effector domain is crucial. It is worth mentioning that no expression system will guarantee the production of high yields of antibody since every molecule comes with its own challenges [85].

5 References

1. Shisana, O., et al., *South African National HIV prevalence, Incidence and Behavior Survey 2012.* HSRC Press, 2014: p. 6-195. .
2. Department, W.H.O.H. *Global summary of the AIDS Epidemic | 2014*. 2015.
3. Barre-Sinoussi, F., et al., *Isolation of a T-lymphotropic retrovirus from a patient at risk for acquired immune deficiency syndrome (AIDS).* Science, 1983. **220**(4599): p. 868-71.
4. Control, C.f.D. *Pneumocystis pneumonia — Los Angeles*. Morbidity and Mortality Weekly Report (MMWR), 1981. **30**, 250-2.
5. Gao, F.e.a., *Origin of HIV-1 in the chimpanzee Pan troglodytes troglodytes.* Nature **397**: p. 436–441.
6. Weiss, R.A., *How does HIV cause AIDS?* Science, 1993. **260**(5112): p. 1273-9.
7. Wilen, C.B., J.C. Tilton, and R.W. Doms, *HIV: cell binding and entry.* Cold Spring Harb Perspect Med, 2012. **2**(8).
8. Fitzon, T., et al., *Proline residues in the HIV-1 NH2-terminal capsid domain: structure determinants for proper core assembly and subsequent steps of early replication.* Virology, 2000. **268**(2): p. 294-307.
9. Engelman, A. and P. Cherepanov, *The structural biology of HIV-1: mechanistic and therapeutic insights.* Nat Rev Microbiol, 2012. **10**(4): p. 279-90.
10. Hurley, J.H. and P.I. Hanson, *Membrane budding and scission by the ESCRT machinery: it's all in the neck.* Nat Rev Mol Cell Biol, 2010. **11**(8): p. 556-66.
11. Briggs, J.A., et al., *Structure and assembly of immature HIV.* Proc Natl Acad Sci U S A, 2009. **106**(27): p. 11090-5.
12. Hartley, O., et al., *V3: HIV's switch-hitter.* AIDS Res Hum Retroviruses, 2005. **21**(2): p. 171-89.
13. Moulard, M., et al., *Selective interactions of polyanions with basic surfaces on human immunodeficiency virus type 1 gp120.* J Virol, 2000. **74**(4): p. 1948-60.
14. Palella, F.J., Jr., et al., *Declining morbidity and mortality among patients with advanced human immunodeficiency virus infection. HIV Outpatient Study Investigators.* N Engl J Med, 1998. **338**((13)): p. p. 853-60.
15. Haqqani, A.A. and J.C. Tilton, *Entry inhibitors and their use in the treatment of HIV-1 infection.* Antiviral Res, 2013. **98**(2): p. 158-70.
16. Chan, D.C., et al., *Core structure of gp41 from the HIV envelope glycoprotein.* Cell, 1997. **89**(2): p. 263-73.
17. Jacobson, J.M., et al., *Safety, pharmacokinetics, and antiretroviral activity of multiple doses of ibalizumab (formerly TNX-355), an anti-CD4 monoclonal antibody, in human immunodeficiency virus type 1-infected adults.* Antimicrob Agents Chemother, 2009. **53**(2): p. 450-7.
18. Kilby, J.M., et al., *The safety, plasma pharmacokinetics, and antiviral activity of subcutaneous enfuvirtide (T-20), a peptide inhibitor of gp41-mediated virus fusion, in HIV-infected adults.* AIDS Res Hum Retroviruses, 2002. **18**(10): p. 685-93.
19. Lalezari, J.P., et al., *A phase II clinical study of the long-term safety and antiviral activity of enfuvirtide-based antiretroviral therapy.* AIDS, 2003. **17**(5): p. 691-8.
20. Dorr, P., et al., *Maraviroc (UK-427,857), a potent, orally bioavailable, and selective small-molecule inhibitor of chemokine receptor CCR5 with broad-spectrum anti-human immunodeficiency virus type 1 activity.* Antimicrob Agents Chemother, 2005. **49**(11): p. 4721-32.
21. Westby, M. and E. van der Ryst, *CCR5 antagonists: host-targeted antivirals for the treatment of HIV infection.* Antivir Chem Chemother, 2005. **16**(6): p. 339-54.

22. Liu, X.D., et al., *Oral administration with attenuated Salmonella encoding a Trichinella cystatin-like protein elicited host immunity.* Exp Parasitol, 2014. **141**: p. 1-11.
23. Iwasaki, A. and R. Medzhitov, *Regulation of adaptive immunity by the innate immune system.* Science, 2010. **327**(5963): p. 291-5.
24. Lipman, N.S., et al., *Monoclonal versus polyclonal antibodies: distinguishing characteristics, applications, and information resources.* ILAR J, 2005. **46**(3): p. 258-68.
25. Broder, S., et al., *NIH conference. T-cell lymphoproliferative syndrome associated with human T-cell leukemia/lymphoma virus.* Ann Intern Med, 1984. **100**(4): p. 543-57.
26. Schur, P.H., *IgG subclasses. A historical perspective.* Monogr Allergy, 1988. **23**: p. 1-11.
27. Vidarsson, G., G. Dekkers, and T. Rispens, *IgG subclasses and allotypes: from structure to effector functions.* Front Immunol, 2014. **5**: p. 520.
28. Ferrante, A., L.J. Beard, and R.G. Feldman, *IgG subclass distribution of antibodies to bacterial and viral antigens.* Pediatr Infect Dis J, 1990. **9**(8 Suppl): p. S16-24.
29. Aalberse, R.C., et al., *IgG4 as a blocking antibody.* Clin Rev Allergy, 1983. **1**(2): p. 289-302.
30. Aalberse, R.C., et al., *Immunoglobulin G4: an odd antibody.* Clin Exp Allergy, 2009. **39**(4): p. 469-77.
31. Polonelli, L., et al., *Antibody complementarity-determining regions (CDRs) can display differential antimicrobial, antiviral and antitumor activities.* PLoS One, 2008. **3**(6): p. e2371.
32. Davies, D.R. and G.H. Cohen, *Interactions of protein antigens with antibodies.* Proc Natl Acad Sci U S A, 1996. **93**(1): p. 7-12.
33. Briney, B.S. and J.E. Jr, *Secondary mechanisms of diversification in the human antibody repertoire.* Front Immunol, 2013. **4**: p. 42.
34. Neuberger, M.S., *Antibody diversification by somatic mutation: from Burnet onwards.* Immunol Cell Biol, 2008. **86**(2): p. 124-32.
35. Brack, C., et al., *A complete immunoglobulin gene is created by somatic recombination.* Cell, 1978. **15**(1): p. 1-14.
36. Oettinger, M.A., et al., *RAG-1 and RAG-2, adjacent genes that synergistically activate V(D)J recombination.* Science, 1990. **248**(4962): p. 1517-23.
37. Kelsoe, G., *B cell diversification and differentiation in the periphery.* J Exp Med, 1994. **180**(1): p. 5-6.
38. Li, Z., et al., *The generation of antibody diversity through somatic hypermutation and class switch recombination.* Genes Dev, 2004. **18**(1): p. 1-11.
39. MacLennan, I.C., *Germinal centers.* Annu Rev Immunol, 1994. **12**: p. 117-39.
40. Casali, P., et al., *DNA repair in antibody somatic hypermutation.* Trends Immunol, 2006. **27**(7): p. 313-21.
41. Zhao, Y., et al., *Two routes for production and purification of Fab fragments in biopharmaceutical discovery research: Papain digestion of mAb and transient expression in mammalian cells.* Protein Expr Purif, 2009. **67**(2): p. 182-9.
42. Andrew, S.M. and J.A. Titus, *Fragmentation of immunoglobulin G.* Curr Protoc Cell Biol, 2003. **Chapter 16**: p. Unit 16 4.
43. Corisdeo, S. and B. Wang, *Functional expression and display of an antibody Fab fragment in Escherichia coli: study of vector designs and culture conditions.* Protein Expr Purif, 2004. **34**(2): p. 270-9.
44. Chadd, H.E. and S.M. Chamow, *Therapeutic antibody expression technology.* Curr Opin Biotechnol, 2001. **12**(2): p. 188-94.
45. Wang, C.A., et al., *Cord blood myeloperoxidase in preterm infants with periventricular hyperechogenicity.* Chang Gung Med J, 2004. **27**(5): p. 337-43.
46. Scolnik, P.A., *mAbs: a business perspective.* MAbs, 2009. **1**(2): p. 179-84.

47. Reichert, J.M., *Monoclonal antibodies as innovative therapeutics.* Curr Pharm Biotechnol, 2008. **9**(6): p. 423-30.
48. Klein, F., et al., *Antibodies in HIV-1 vaccine development and therapy.* Science, 2013. **341**(6151): p. 1199-204.
49. Scott, A.M., J.D. Wolchok, and L.J. Old, *Antibody therapy of cancer.* Nat Rev Cancer, 2012. **12**(4): p. 278-87.
50. Weiner, L.M., R. Surana, and S. Wang, *Monoclonal antibodies: versatile platforms for cancer immunotherapy.* Nat Rev Immunol, 2010. **10**(5): p. 317-27.
51. Ecker, D.M., S.D. Jones, and H.L. Levine, *The therapeutic monoclonal antibody market.* MAbs, 2015. **7**(1): p. 9-14.
52. Cai, H.H., *Therapeutic Monoclonal Antibodies Approved by FDA in 2015.* MOJ Immunol, 2016. **3**(2): p. 1-2.
53. Doig, A.R., Ecker, D. M. and Ransohoff, T., C. , *Monoclonal Antibody Targets and Indications.* American Pharmaceutical review, 2015: p. 1-8.
54. Gaschen, B., et al., *Diversity considerations in HIV-1 vaccine selection.* Science, 2002. **296**(5577): p. 2354-60.
55. Doria-Rose, N.A., et al., *Frequency and phenotype of human immunodeficiency virus envelope-specific B cells from patients with broadly cross-neutralizing antibodies.* J Virol, 2009. **83**(1): p. 188-99.
56. Sun, Z., et al., *Reconstitution and characterization of antibody repertoires of HIV-1-infected "elite neutralizers".* Antiviral Res, 2015. **118**: p. 1-9.
57. Kwong, P.D. and J.R. Mascola, *Human antibodies that neutralize HIV-1: identification, structures, and B cell ontogenies.* Immunity, 2012. **37**(3): p. 412-25.
58. Huang, J., et al., *Broad and potent HIV-1 neutralization by a human antibody that binds the gp41-gp120 interface.* Nature, 2014. **515**(7525): p. 138-42.
59. Scharf, L., et al., *Antibody 8ANC195 reveals a site of broad vulnerability on the HIV-1 envelope spike.* Cell Rep, 2014. **7**(3): p. 785-95.
60. Falkowska, E., et al., *Broadly neutralizing HIV antibodies define a glycan-dependent epitope on the prefusion conformation of gp41 on cleaved envelope trimers.* Immunity, 2014. **40**(5): p. 657-68.
61. Blattner, C., et al., *Structural delineation of a quaternary, cleavage-dependent epitope at the gp41-gp120 interface on intact HIV-1 Env trimers.* Immunity, 2014. **40**(5): p. 669-80.
62. Lee, J.H., et al., *Antibodies to a conformational epitope on gp41 neutralize HIV-1 by destabilizing the Env spike.* Nat Commun, 2015. **6**: p. 8167.
63. West, A.P., Jr., et al., *Structural insights on the role of antibodies in HIV-1 vaccine and therapy.* Cell, 2014. **156**(4): p. 633-48.
64. Zhou, T., et al., *Structural basis for broad and potent neutralization of HIV-1 by antibody VRC01.* Science, 2010. **329**(5993): p. 811-7.
65. Scheid, J.F., et al., *Broad diversity of neutralizing antibodies isolated from memory B cells in HIV-infected individuals.* Nature, 2009. **458**(7238): p. 636-40.
66. Diskin, R., et al., *Increasing the potency and breadth of an HIV antibody by using structure-based rational design.* Science, 2011. **334**(6060): p. 1289-93.
67. West, A.P., Jr., et al., *Structural basis for germ-line gene usage of a potent class of antibodies targeting the CD4-binding site of HIV-1 gp120.* Proc Natl Acad Sci U S A, 2012. **109**(30): p. E2083-90.
68. Scheid, J.F., et al., *Sequence and structural convergence of broad and potent HIV antibodies that mimic CD4 binding.* Science, 2011. **333**(6049): p. 1633-7.

69. Burkly, L.C., et al., *Inhibition of HIV infection by a novel CD4 domain 2-specific monoclonal antibody. Dissecting the basis for its inhibitory effect on HIV-induced cell fusion.* J Immunol, 1992. **149**(5): p. 1779-87.
70. Holling, T.M., E. Schooten, and P.J. van Den Elsen, *Function and regulation of MHC class II molecules in T-lymphocytes: of mice and men.* Hum Immunol, 2004. **65**(4): p. 282-90.
71. Littman, D.R., *The structure of the CD4 and CD8 genes.* Annu Rev Immunol, 1987. **5**: p. 561-84.
72. Maddon, P.J., et al., *The isolation and nucleotide sequence of a cDNA encoding the T cell surface protein T4: a new member of the immunoglobulin gene family.* Cell, 1985. **42**(1): p. 93-104.
73. Xu, H. and D.R. Littman, *A kinase-independent function of Lck in potentiating antigen-specific T cell activation.* Cell, 1993. **74**(4): p. 633-43.
74. Moore, J.P., et al., *A monoclonal antibody to CD4 domain 2 blocks soluble CD4-induced conformational changes in the envelope glycoproteins of human immunodeficiency virus type 1 (HIV-1) and HIV-1 infection of CD4+ cells.* J Virol, 1992. **66**(8): p. 4784-93.
75. Freeman, M.M., et al., *Crystal structure of HIV-1 primary receptor CD4 in complex with a potent antiviral antibody.* Structure, 2010. **18**(12): p. 1632-41.
76. Boon, L., et al., *Development of anti-CD4 MAb hu5A8 for treatment of HIV-1 infection: preclinical assessment in non-human primates.* Toxicology, 2002. **172**(3): p. 191-203.
77. Kuritzkes, D.R., et al., *Antiretroviral activity of the anti-CD4 monoclonal antibody TNX-355 in patients infected with HIV type 1.* J Infect Dis, 2004. **189**(2): p. 286-91.
78. Bruno, C.J. and J.M. Jacobson, *Ibalizumab: an anti-CD4 monoclonal antibody for the treatment of HIV-1 infection.* J Antimicrob Chemother, 2010. **65**(9): p. 1839-41.
79. Norris, D., Morales, J., Gathe, J. et. al., *Phase 2 efficacy and safety of the novel entry inhibitor, TNX-355, in combination with optimized background regimen (OBR).* Abstracts of the Sixteenth International AIDS Conference. International AIDS Society, 2006.
80. Delmonico, F.L., et al., *Immunosuppression of cynomolgus renal allograft recipients with humanized OKT4A monoclonal antibodies.* Transplant Proc, 1993. **25**(1 Pt 1): p. 784-5.
81. Pace, C.S., et al., *Bispecific antibodies directed to CD4 domain 2 and HIV envelope exhibit exceptional breadth and picomolar potency against HIV-1.* Proc Natl Acad Sci U S A, 2013. **110**(33): p. 13540-5.
82. Drees, J.J., et al., *Soluble production of a biologically active single-chain antibody against murine PD-L1 in Escherichia coli.* Protein Expr Purif, 2014. **94**: p. 60-6.
83. Antman, E.M., et al., *Treatment of 150 cases of life-threatening digitalis intoxication with digoxin-specific Fab antibody fragments. Final report of a multicenter study.* Circulation, 1990. **81**(6): p. 1744-52.
84. Pizon, A.F., et al., *Safety and efficacy of Crotalidae Polyvalent Immune Fab in pediatric crotaline envenomations.* Acad Emerg Med, 2007. **14**(4): p. 373-6.
85. Frenzel, A., M. Hust, and T. Schirrmann, *Expression of recombinant antibodies.* Front Immunol, 2013. **4**: p. 217.
86. Kirsch, M., et al., *Parameters affecting the display of antibodies on phage.* J Immunol Methods, 2005. **301**(1-2): p. 173-85.
87. Li, J., et al., *A comparative study of different vector designs for the mammalian expression of recombinant IgG antibodies.* J Immunol Methods, 2007. **318**(1-2): p. 113-24.
88. Laemmli, U.K., *Cleavage of structural proteins during the assembly of the head of bacteriophage T4.* Nature, 1970. **227**(5259): p. 680-5.
89. Cerutti, N., et al., *Stabilization of HIV-1 gp120-CD4 receptor complex through targeted interchain disulfide exchange.* J Biol Chem, 2010. **285**(33): p. 25743-52.

90. Li, M., et al., *Human immunodeficiency virus type 1 env clones from acute and early subtype B infections for standardized assessments of vaccine-elicited neutralizing antibodies.* J Virol, 2005. **79**(16): p. 10108-25.
91. Nesbeth, D.N., et al., *Growth and productivity impacts of periplasmic nuclease expression in an Escherichia coli Fab' fragment production strain.* Biotechnol Bioeng, 2012. **109**(2): p. 517-27.
92. Cooke, G.D., et al., *A modified Escherichia coli protein production strain expressing staphylococcal nuclease, capable of auto-hydrolysing host nucleic acid.* J Biotechnol, 2003. **101**(3): p. 229-39.
93. Trkola, A., et al., *Human monoclonal antibody 2G12 defines a distinctive neutralization epitope on the gp120 glycoprotein of human immunodeficiency virus type 1.* J Virol, 1996. **70**(2): p. 1100-8.
94. Sanders, R.W., et al., *The mannose-dependent epitope for neutralizing antibody 2G12 on human immunodeficiency virus type 1 glycoprotein gp120.* J Virol, 2002. **76**(14): p. 7293-305.
95. Pace, C.S., et al., *Anti-CD4 monoclonal antibody ibalizumab exhibits breadth and potency against HIV-1, with natural resistance mediated by the loss of a V5 glycan in envelope.* J Acquir Immune Defic Syndr, 2013. **62**(1): p. 1-9.
96. Inc, T.B., *A Phase 3, Single Arm, 24-Week, Multicenter Study of Ibalizumab Plus an Optimized Background Regimen (OBR) in Treatment-Experienced Patients Infected With Multi-Drug Resistant HIV-1.* In: ClinicalTrials.gov. Bethesda (MD): National Library of Medicine (US) NLM Identifier: NCT02475629, June 11, 2015.
97. Levy, R., et al., *Production of correctly folded Fab antibody fragment in the cytoplasm of Escherichia coli trxB gor mutants via the coexpression of molecular chaperones.* Protein Expr Purif, 2001. **23**(2): p. 338-47.
98. Baeshen, N.A., et al., *Cell factories for insulin production.* Microb Cell Fact, 2014. **13**: p. 141.
99. Chan, C.E., et al., *Optimized expression of full-length IgG1 antibody in a common E. coli strain.* PLoS One, 2010. **5**(4): p. e10261.
100. Yoon, S.H., S.K. Kim, and J.F. Kim, *Secretory production of recombinant proteins in Escherichia coli.* Recent Pat Biotechnol, 2010. **4**(1): p. 23-9.
101. Sockolosky, J.T. and F.C. Szoka, *Periplasmic production via the pET expression system of soluble, bioactive human growth hormone.* Protein Expr Purif, 2013. **87**(2): p. 129-35.
102. Berkmen, M., *Production of disulfide-bonded proteins in Escherichia coli.* Protein Expr Purif, 2012. **82**(1): p. 240-51.
103. Selleck, W. and S. Tan, *Recombinant protein complex expression in E. coli.* Curr Protoc Protein Sci, 2008. **Chapter 5**: p. Unit 5 21.
104. Bowering, L.C., et al., *Comparison of techniques for monitoring antibody fragment production in E. coli fermentation cultures.* Biotechnol Prog, 2002. **18**(6): p. 1431-8.
105. Better, M., et al., *Escherichia coli secretion of an active chimeric antibody fragment.* Science, 1988. **240**(4855): p. 1041-3.
106. Venturi, M., C. Seifert, and C. Hunte, *High level production of functional antibody Fab fragments in an oxidizing bacterial cytoplasm.* J Mol Biol, 2002. **315**(1): p. 1-8.
107. Donovan, R.S., C.W. Robinson, and B.R. Glick, *Optimizing the expression of a monoclonal antibody fragment under the transcriptional control of the Escherichia coli lac promoter.* Can J Microbiol, 2000. **46**(6): p. 532-41.
108. Bothmann, H. and A. Pluckthun, *Selection for a periplasmic factor improving phage display and functional periplasmic expression.* Nat Biotechnol, 1998. **16**(4): p. 376-80.
109. Chen, R. and U. Henning, *A periplasmic protein (Skp) of Escherichia coli selectively binds a class of outer membrane proteins.* Mol Microbiol, 1996. **19**(6): p. 1287-94.

110. Hohenblum, H., et al., *Bacterial expression and refolding of human trypsinogen.* J Biotechnol, 2004. **109**(1-2): p. 3-11.
111. Laemmli, U.K., F. Beguin, and G. Gujer-Kellenberger, *A factor preventing the major head protein of bacteriophage T4 from random aggregation.* J Mol Biol, 1970. **47**(1): p. 69-85.
112. De Pourcq, K., et al., *Engineering the yeast Yarrowia lipolytica for the production of therapeutic proteins homogeneously glycosylated with Man(8)GlcNAc(2) and Man(5)GlcNAc(2).* Microb Cell Fact, 2012. **11**: p. 53.
113. Basile, G. and M. Peticca, *Recombinant protein expression in Leishmania tarentolae.* Mol Biotechnol, 2009. **43**(3): p. 273-8.
114. Niimi, T., *Recombinant protein production in the eukaryotic protozoan parasite Leishmania tarentolae: a review.* Methods Mol Biol, 2012. **824**: p. 307-15.
115. Breitling, R., et al., *Non-pathogenic trypanosomatid protozoa as a platform for protein research and production.* Protein Expr Purif, 2002. **25**(2): p. 209-18.
116. Breton, M., et al., *A recombinant non-pathogenic Leishmania vaccine expressing human immunodeficiency virus 1 (HIV-1) Gag elicits cell-mediated immunity in mice and decreases HIV-1 replication in human tonsillar tissue following exposure to HIV-1 infection.* J Gen Virol, 2007. **88**(Pt 1): p. 217-25.
117. Klatt, S., et al., *Production of glycosylated soluble amyloid precursor protein alpha (sAPPalpha) in Leishmania tarentolae.* J Proteome Res, 2013. **12**(1): p. 396-403.
118. Klatt, S. and Z. Konthur, *Secretory signal peptide modification for optimized antibody-fragment expression-secretion in Leishmania tarentolae.* Microb Cell Fact, 2012. **11**: p. 97.
119. Ko, K., *Expression of recombinant vaccines and antibodies in plants.* Monoclon Antib Immunodiagn Immunother, 2014. **33**(3): p. 192-8.
120. Daniell, H., S.J. Streatfield, and K. Wycoff, *Medical molecular farming: production of antibodies, biopharmaceuticals and edible vaccines in plants.* Trends Plant Sci, 2001. **6**(5): p. 219-26.
121. Stoger, E., et al., *Recent progress in plantibody technology.* Curr Pharm Des, 2005. **11**(19): p. 2439-57.
122. Karasev, A.V., et al., *Plant based HIV-1 vaccine candidate: Tat protein produced in spinach.* Vaccine, 2005. **23**(15): p. 1875-80.
123. Koser, M.L., et al., *Rabies virus nucleoprotein as a carrier for foreign antigens.* Proc Natl Acad Sci U S A, 2004. **101**(25): p. 9405-10.
124. Golovkin, M., Spitsin, S., Andrianov, V. et. al, *Smallpox subunit vaccine produced in Planta confers protection in mice.* Proc Natl Acad Sci, 2007(104): p. 6864–6869.
125. Bandurska, K., Brodzik, R., Spitsin, S. et. al, *Plant-produced hepatitis B core protein chimera carrying anthrax protective antigen domain-4.* Hybridoma, 2008(27): p. 241-247.
126. Pogrebnyak, N., et al., *Severe acute respiratory syndrome (SARS) S protein production in plants: development of recombinant vaccine.* Proc Natl Acad Sci U S A, 2005. **102**(25): p. 9062-7.
127. Ma, J.K., et al., *Regulatory approval and a first-in-human phase I clinical trial of a monoclonal antibody produced in transgenic tobacco plants.* Plant Biotechnol J, 2015. **13**(8): p. 1106-20.
128. Shattock, R.J. and J.P. Moore, *Inhibiting sexual transmission of HIV-1 infection.* Nat Rev Microbiol, 2003. **1**(1): p. 25-34.

6 Ethics

Human Research Ethics Committee (Medical)

Research Office Secretariat: Senate House Room SH10005, 10th floor. Tel +27 (0)11-717-1252
Medical School Secretariat: Tobias Health Sciences Building, 2nd floor Tel +27 (0)11-717-2700
Private Bag 3, Wits 2050, www.wits.ac.za. Fax +27 (0)11-717-1265

Ref: W-CJ-150615-2 15/06/2015

***TO WHOM IT MAY CONCERN*:**

Waiver: This certifies that the following research does not require clearance from the Human Research Ethics Committee (Medical).

Investigator: **Ms R Munshi, Dr N Cerutti, Dr A Capovilla.**

Project title: **The expression and purification of the F(ab) fragment of Ibalizumab: a monoclonal anti-CD4 antibody with potent HIV inhibitory effects.**

Reason: This *in vitro* laboratory study will use stored E.coli as an alternative cost-effective production platform. There are no human participants

Professor Peter Cleaton-Jones

Chair: Human Research Ethics Committee (Medical)

Copy – HREC (Medical) Secretariat: Zanele Ndlovu, Langutani Masingi.

Appendix 1: Customary Protocols and Recipes

Solutions for bacterial culture

Luria-Bertani (LB) Broth (1L)

10 g Tryptone powder (OxoidInc; Basingstoke, Hampshire, England), 5 g of yeast extract powder (BioLab; Wadeville, Gauteng, South Africa) and 5 g of NaCl were dissolved in dH_2O to a final volume of 1 L. the broth was autoclaved at 121˚C, 1 kg/cm^2 for 20 minutes and stored at ambient temperature until use.

Agar plates

7 g of agar powder was added to 200 ml of dH_2O and autoclaved at 121˚C, 1 kg/cm^2 for 20 minutes and stored at ambient temperature until use. When used the agar was warmed in the microwave and the appropriate antibiotics were added at 100 mg/ml, poured into 90 mmm petri dishes and allowed to set.

Ampicillin stock (100 mg/ml)

1 g of ampicillin (Sigma-Aldrich; Germany) was dissolved in 70 % Ethanaol to a final volume of 10 ml and stored at -20˚C until use.

Transformation buffer (100mls) (for chemically competent cells)

1.4702 g of $CaCl_2.H_2O$ (100 mM), 0.3024 g of PIPES.HCl (10mM) (Boehringer Mannheim; GmBh, Germany) and 15ml glycerol (15 %) were mixed with dH_2O to a final volume of 100 ml. the pH of the solution was adjusted to 7.0 using 10 M NaOH. The solution was then autoclaved and stored at -20˚C until use.

Preparation of competent bacterial cell (DH5α and BL21 (DE3) stars

20 ml of LB broth was inoculated with 10 µl of DH5α (Novagen; Germany) and BL21 (DE3) stars stock, under sterile conditions. The cultures were incubated overnight at 37˚C in an orbital shaker. The overnight cultures were diluted 1:40 in LB broth and grown for 2 to 3 hours at 37˚C in an orbital shaker to stimulate log phase growth. Once the A_{600} readings reached 0.4, cells were then harvested at 1000 x *g* for 20 minutes at 4˚C. The cell pellet was then resuspended in 10 ml ice cold transformation buffer and incubated on ice for 20 minutes. The cells were then harvested

once again and the cell pellet resuspended in 1 ml transformation buffer. 100 µl aliquots were prepared, snap-forzen in acetone and dry ice then stored at -80˚C until use.

Transformation of competent E. coli cells

1 µl (~50 ng) of plasmid DNA or 10 µl of ligation reaction was added to 50 µl of competent E. coli, the mixture was incubated on ice for 20 to 25 minutes. A negative control was set alongside, containing no plasmid DNA. Cells were heat shocked at 42˚C for 30 seconds and immediately incubated on ice for 2 minutes. Each transformation reaction was spread onto an agar plate with the appropriate antibiotic, under sterile conditions and incubated at 37˚C overnight.

Solutions for Agarose Electrophoresis

0.5 M EDTA (Ethelynedianine Tetra-acetic Acid) (pH 8.0)

93.05 g of EDTA powder was dissolved in dH_2O to a final volume of 500 ml. The pH was adjusted to 8.0 using 10 M NaOH. It was autoclaved and stored at room temperature until use.

50 x TAE Buffer

242 g Tris base, 57.1 ml glacial acetic acid and 100 ml 0.5 M EDTA were added to dH_2O to a final volume of 1 L and stored at room temperature until use. The solution was diluted to a 1 x buffer before use using dH_2O.

Preparation of agarose gels

0.8 % or 1 % agarose gels were prepared by adding either 0.8 or 1 g of agarose powder to 100 ml of 1 x TAE buffer. The mixture was then heated until the agarose dissolved. Before pouring the gels, 5 µl of ethidium bromide (Promega; Madison, WI) was added. Gels were poured and allowed to set in a Bio-Rad Gel chamber system (Bio-Rad; Gercules, CA).

Electrophoresis Procedure

The agrose gels were resolved in a Bio-Rad Gel Tank system (Bio-Rad; Hercules, CA) and submerged in 1 x TAE buffer, allowing for even heat conduction. All DNA samples, comtrols and DNA ladder wer mixed with DNA loading buffer. The voltage was set at 30 V till the samples had keft the wells and increased to 80 V until the gel had completely resolved. DNA bands on the gels

were visualized using a Universal Hood Gel Doc and the Quantity One Software Programme (Bio-Rad; Hercules, CA).

Protein purification

Solutions for protein Purification of 2dCD4

M Nickel Sulphate ($NiSO_4$)

5.257 g of $NiSO_4$ was added to 200 ml dH_2O and stored at room temperature until use.

2 M Sodium Hydroxide (NaOH)

8 g of NaOH was dissolved in 100 ml of dH_2O, autoclaved and stored at room temperature until use.

0 mM Imidazole purification buffer

1.86 g of glycine, 70 µl of β-mercaptaethanol, 14.61 g NaCl and 240 g of urea were mixed in dH_2O until a final volume of 500 ml was reached. The buffer was stored at room temperature until use.

500 mM Imidazole buffer (pH 7.4)

1.86 g of glycine, 70 µl of β-mercaptaethanol, 14.61 g NaCl, 17 g of imidazole powder and 240 g of urea were mixed in dH_2O until a final volume of 500 ml was reached. The buffer was stored at room temperature until use.

In vitro Folding Buffer A (pH 9.6)

3.75 g glycine, 100 g sucrose, 2 ml 0.5 M EDTA, 0.31 g GSH, 0.06 g GSSG, 240 g urea and 2.8 ml 2M NaOH were mixed in Milliq water until a final volume of 1 L was reached. The solution was made prior to folding.

In vitro Folding Buffer B (pH 9.6)

1.59 g of Sodium Carbonate, 2.93 g of Sodium Bicarbonate, 100 g sucrose, 2 ml 0.5 M EDTA, 0.031 g GSH and 0.006 g GSSG were mixed in MilliQ water until a final volume of 1 L was reached. The solution was made prior to folding.

Preparation of columns for purification procedures

Nickel-charged sepharose 6B resin was used to purify 2dCD4. The histidine tag attached to the C-terminal end associated with the charged nickel resin. Two 15 ml falcon tubes with 1 ml of packed resin were washed with dH_2O three times and centrifuges at 3500 rpm for 5 minutes. Ten milliliters of 0.1 M $NiSO_4$ solution was added to each tube and incubated for 15 minutes at room temperature with gentle agitation. The resin was then centrifuged as previously described, the supernatant then removed, and washed with dH_2O three more times.

Solutions for Denaturing Discontinuous Electrophoresis

Monomer solution

30 g of acrylamide, 0.8 g of N, N' – methylene bisacylamide was dissolved in dH_2O to a final volume of 100 ml. the solution was stored at 4˚C in the dark until use.

4 x running gel buffer (pH 8.8)

91 g of Tris/HCl was dissolved in dH_2O to a final volume of 500 ml. The pH was adjusted to 8.8 with HCl and stored at 4˚C in the dark until use.

4 x stacking gel buffer (pH 6.8)

6.05 g of Tris/HCl was dissolved in dH_2O to a final volume of 100 ml. The pH was adjusted to 8.8 with HCl and stored at 4˚C in the dark until use.

10 % Sodium Dodecyl Sulphate (SDS)

10 g of SDS was dissolved in dH_2O to a final volume of 100 ml. the solution was stored at room temperature until use.

10 % ammonium persulphate (APS)

0.1 g of APS was dissolved in dH_2O to a final volume of 1 ml. APS was made fresh as needed.

Preparation of SDS-PAGE gels

12.5 % running gel solution (2 gels)

12.5 ml of monomer solution, 7.5 ml 4 x running buffer, 0.3 ml 10 % SDS and 9.6 ml dH_2O were mixed, before casting the gels 150 µl of APS and 10 µl tetramethylethylenediamine (TEMED) (Sigma-Aldrich; Steinheim, Germany) were added to the solution.

Stacking gel solution (2 gels)

For a gel thickness of 0.75 mm: 1.33 ml of monomer solution, 2.5 ml 4 x stacking buffer, 0.1 ml 10 % SDS and 6 ml dH_2O were mixed, before casting the gels 50 µl of APS and 5 µl of TEMED were added to the solution.

Reducing Sample buffer (2 X)

2.5 ml 4 x stacking buffer, 4 ml 10 % SDS, 2 ml glycerol, 2 mg bromophenol blue (Saarchem; Merck chemicals, Wadeville, SA) and 0.2 ml β-mercaptaethanol were mixed with dH_2O to a final volume of 10 ml. aliquots of 1 ml were stored at -20˚C until use.

10 X Tank Buffer

30.28 g of Tris/HCl, 144.13 g glycine and 10 g SDS were mixed with dH_2O to a final volume of 1 liter. The solution was stored at room temperature until use.

Casting of SDS-PAGE gels

Denaturing PAGE gels were cast using a BioRad gel casting system (BioRad; Hercules, CA). The casting chamber was assembled and sealed, running gel solution was added to each chamber and a layer of isopropanol added to seal and level out the gels. Once polymerized, the isopropanol was removed and the stacking gel solution added. The gels were allowed to polymerize before being sealed in an airtight bag and stored at 4˚C for up to 2 weeks or until use.

Electrophoresis procedure

Gels were resolved under denaturing conditions using the BioRad Gel System (BioRad; Hercules, CA) submerged in 1 x Tank buffer, allowing for even heat conduction. All protein samples and comtrols were treated with 2 x reducing sample buffer or non-reducing buffer. The protein and sample buffer mix was incubated at ~80˚C for 5 minutes, to allow for denaturation of the protein,

before being loaded into the wells of the gels. Gesl were run at 10 mA per gel till the samples were stacked and at 25 mA per gel to resolve the samples.

Staining procedures

Coomassie staining solution

0.25 g of Coomassie® Brilliant Blue R250 (Sigma-Aldrich; Steinheim, Germany) was dissolved in 500 ml of methanol, 100 ml acetic acid and 400 ml dH_2O. The solution was stored at room temperature until use.

De-staining solution

400 ml methanol, 70 ml acetic acid and 530 ml dH_2O were mixed and stored at room temperature until use.

Protocol for de-staining procedures

SDS-PAGE gels were stained with Coomassie® Brilliant Blue R-250 solution overnight at room temperature with gentle agitation. The gels were then de-stained overnight with de-staining solution at room temperature overnight with gentle agitation. Protein bands were visualized under white light using a Universal Gel Doc hood (BioRad; Hercules, CA) and images were captured using the Quantity One Version Software Program.

Western blotting solutions and procedure

Transfer buffer

200 ml methanol, 100 ml 10 x Tank buffer and 700 ml dH_2O were mixed and stored at room temperature until use.

10 x Tris-Buffered Saline (TBS)

160 g NaCl, 4 g KCl and 60 g Tris/HCl were dissolved in dH_2O to a final volume of 2 liters. HCl was used to adjust the pH of the solution. The solution was autoclaved and stored at room temperature until use.

T-TBS

Just before use, 10 x TBS was diluted 1:10 with dH_2O and Tween 20® (Sigma-Aldrich; Steinheim, Germany) was added to a final concentration of 0.1 % (v/v).

Blocking buffer (5 %)

2.5 g fat free casein milk powder solution in 50 ml T-TBS.

Western blotting Procedures

SDS-PAGE gels and nitrocellulose membranes were equilibrated in Transfer buffer and placed on the Trans-Blot apparatus. Transfer conditions were set at 20 volts and the between 40 – 180 mA (depending on the amount of gels being transferred) for 30 minutes. Following protein transfer, the nitrocellulose membrane was blocked in blocking buffer for 1 hour with gentle agitation or overnight at 4˚C. The blocking buffer was then removed and the membrane probed with either a HRP-conjugated his-probe or HRP-conjugated anti-kappa light chain specific antibody for 1 hour at room temperature. The nitrocellulose membrane was washed 3 times, for 5 minutes each, with T-TBS on a shaker to remove any unbound antibody. Protein detection was performed by standard chemiluminescence methods. Protein bands were using a Universal Gel Doc hood (BioRad; Hercules, CA) and images were captured using the Quantity One Version Software Program.

Standard chemiluminescence Methods

Equal volumes of Stable Peroxide solution and Luminol/Enhancer Solution from the SuperSignal® West Pico Chemiluminescent Substrate Kit (Peirce; Rockford, IL, USA) were mixed and added to the membrane for 5 minutes at room temperature.

BCA Assay (Thermo Fisher Scientific; Massachusetts, USA)

Concentration determination was achieved by means of the Bradford assay making use of the BCA assay kit. The experiment was carried out according to the manufacturer's instructions. Bovine Serum Albumin standards were run alongside each sample being quantified. Concentrations of the standards ranged from 2000 – 0 μg/ml. Samples of 25μl of the standards and protein of interest were aliquoted in duplicate. A volume of 200 μl of working reagent was added to each well and allowed to incubate at 56 °C for 30 minutes. Absorbance readings at 570 nm were determined spectrophotometrically and the concentrations calculated using the *LX-560* microplate software.

Appendix 2: Nucleotide sequence of recombinant Ibalizumab Fab Fragment and pET15b Expression vector

Nucleotide sequence of recombinant Ibalizumab Fab Fragment

```
CACTATAGGGCGAATTGAAGGAAGGCCGTCAAGGCCGCATTCATGAAAAAAACCGCAATT
1 ---------+---------+---------+---------+---------+---------+
ompA                                                Ibalizumab Light chain
GCCATTGCAGTTGCACTGGCAGGTTTTGCAACCGTTGCACAGGCAGATATTGTTATGACC
61 ---------+---------+---------+---------+---------+---------+

CAGAGTCCGGATAGCCTGGCAGTTAGCCTGGGTGAACGTGTTACCATGAATTGTAAAAGC
121 ---------+---------+---------+---------+---------+---------+

AGCCAGAGCCTGCTGTATAGCACCAATCAGAAAAACTATCTGGCATGGTATCAGCAGAAA
181 ---------+---------+---------+---------+---------+---------+

CCGGGTCAGAGCCCGAAACTGCTGATTTATTGGGCAAGCACCCGTGAAAGCGGTGTTCCG
241 ---------+---------+---------+---------+---------+---------+

GATCGTTTTAGCGGTAGCGGTAGTGGCACCGATTTTACCCTGACCATTAGCAGCGTTCAG
301 ---------+---------+---------+---------+---------+---------+

GCAGAGGATGTTGCAGTGTATTATTGTCAGCAGTATTATAGCTATCGCACCTTTGGTGGT
361 ---------+---------+---------+---------+---------+---------+

GGCACCAAACTGGAAATTAAACGTACCGTTGCAGCACCGAGCGTTTTTATCTTTCCGCCT
421 ---------+---------+---------+---------+---------+---------+

AGTGATGAACAGCTGAAAAGCGGCACCGCAAGCGTTGTTTGTCTGCTGAATAACTTTTAT
481 ---------+---------+---------+---------+---------+---------+

CCGCGTGAAGCAAAAGTTCAGTGGAAAGTTGATAATGCACTGCAGAGCGGTAATAGCCAA
541 ---------+---------+---------+---------+---------+---------+

GAAAGCGTTACCGAACAGGATAGCAAAGATAGCACCTATAGCCTGAGCAGCACCCTGACC
601 ---------+---------+---------+---------+---------+---------+

CTGAGCAAAGCAGATTATGAAAAACACAAAGTGTATGCCTGCGAAGTTACCCATCAGGGT
661 ---------+---------+---------+---------+---------+---------+
```

CTGAGCAGTCCGGTTACCAAAAGCTTTAATCGTGGTGAATGCTAATAATCTAGAAATAAT
721 ---------+---------+---------+---------+---------+---------+

RBS

TTTGTTTAACTTTAAGAAGGAGATATACATATGAAATATCTGCTGCCGACCGCAGCAGCG
781 ---------+---------+---------+---------+---------+---------+

6x Histidine tag

GGTCTGCTGCTGCTGGCAGCACAGCCTGCAATGGCACATCATCATCATCACCATGGTAGC
841 ---------+---------+---------+---------+---------+---------+

Ibalizumab Heavy chain

GGTAGCCAGGTTCAGCTGCAGCAGAGCGGTCCGGAAGTTGTTAAACCGGGTGCAAGCGTT
901 ---------+---------+---------+---------+---------+---------+

AAAATGAGCTGTAAAGCAAGCGGTTATACCTTTACCAGCTATGTTATTCATTGGGTTCGT
961 ---------+---------+---------+---------+---------+---------+

CAGAAACCTGGTCAGGGTCTGGATTGGATTGGTTATATCAATCCGTATAATGATGGCACC
1021 ---------+---------+---------+---------+---------+---------
+

GATTATGATGAAAAATTCAAAGGTAAAGCAACCCTGACCAGCGATACCAGCACCAGCACC
1081 ---------+---------+---------+---------+---------+---------
+

GCATATATGGAACTGAGCAGCCTGCGTAGCGAAGATACAGCCGTGTATTATTGCGCACGT
1141 ---------+---------+---------+---------+---------+---------
+

GAGAAAGATAATTATGCAACCGGTGCATGGTTTGCATATTGGGGTCAGGGCACCCTGGTT
1201 ---------+---------+---------+---------+---------+---------
+

ACCGTTAGCAGCGCAAGCACCAAAGGTCCGAGCGTGTTTCCGCTGGCACCGAGCAGCAAA
1261 ---------+---------+---------+---------+---------+---------
+

AGCACCAGCGGTGGCACCGCAGCACTGGGTTGTCTGGTTAAAGATTATTTTCCGGAACCG
1321 ---------+---------+---------+---------+---------+---------
+

GTTACCGTGAGCTGGAATAGCGGTGCACTGACCAGCGGTGTTCATACCTTTCCGGCAGTT
1381 ---------+---------+---------+---------+---------+---------
+

CTGCAGAGCAGCGGTCTGTATAGCCTGAGTAGCGTTGTTACCGTTCCGAGCAGCAGCCTG

```
1441 ---------+---------+---------+---------+---------+---------
+

GGCACCCAGACCTATATTTGTAATGTTAATCATAAACCGAGCAATACCAAAGTGGACAAA
1501 ---------+---------+---------+---------+---------+---------
+

AAAGCAGAACCGAAAAGCTGCTAATAACTCGAGGATCCCTGGGCCTCATGGGCCTTCCTT
```

pET15b Expression vector of the recombinant Ibalizumab Fab fragment

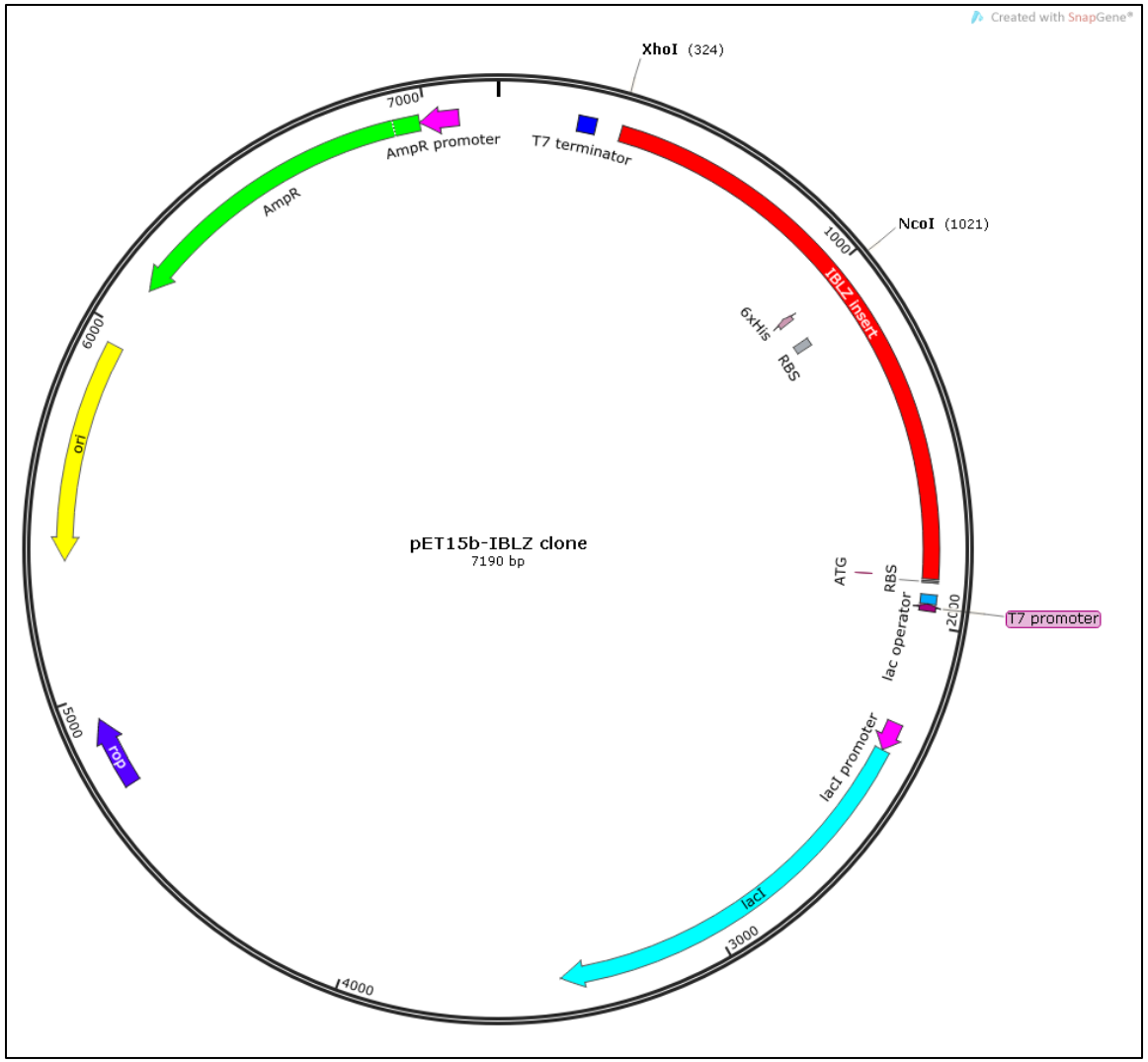

Sequence similarity of Ibalizumab Fab fragment construct

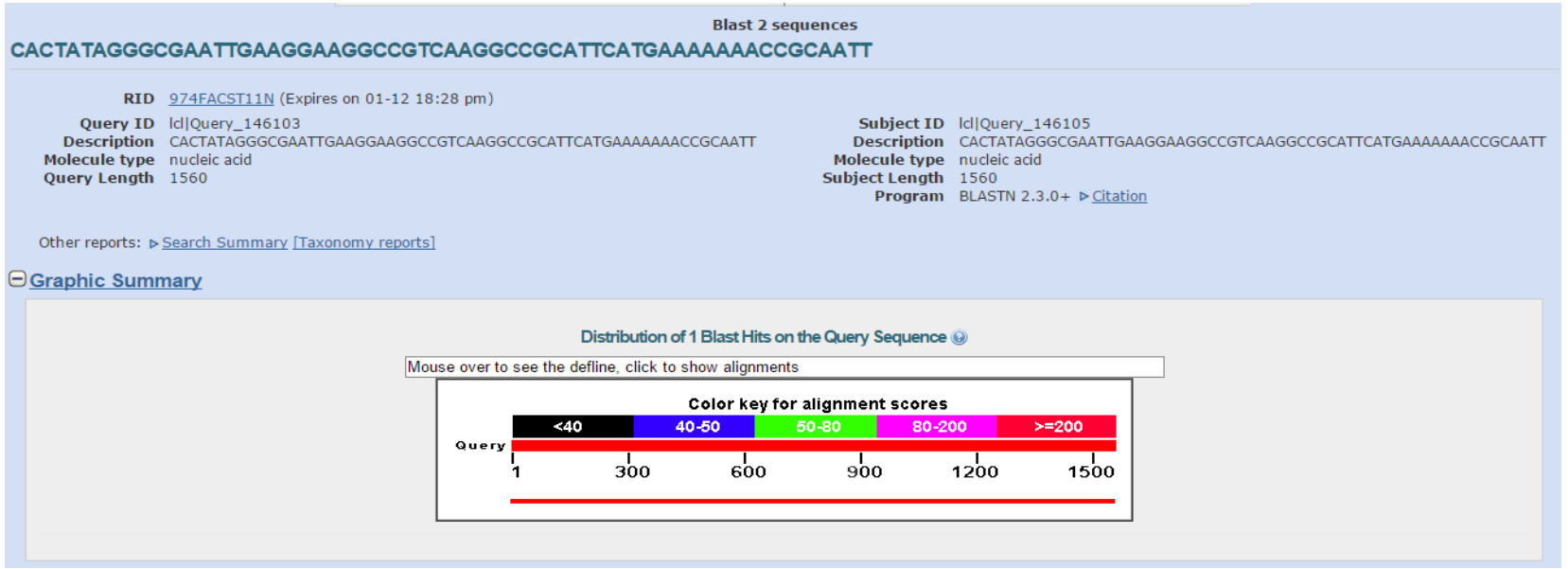

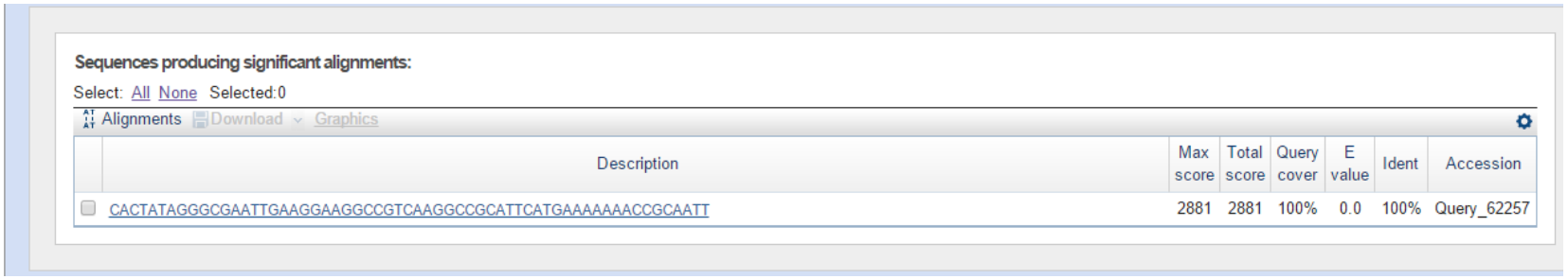

Sequencing result of sub-cloned Ibalizumab Fab fragment construct

The sequence alignment was completed using the NCBI alignment tool (blast.ncbi.nlm.nih.gov/BLAST.cgi). Expression plasmids were sequenced and aligned to the parent insert strand. Sequence similarity of 100 % was achieved (bottom right hand corner).

Appendix 3: Supplementary Figures

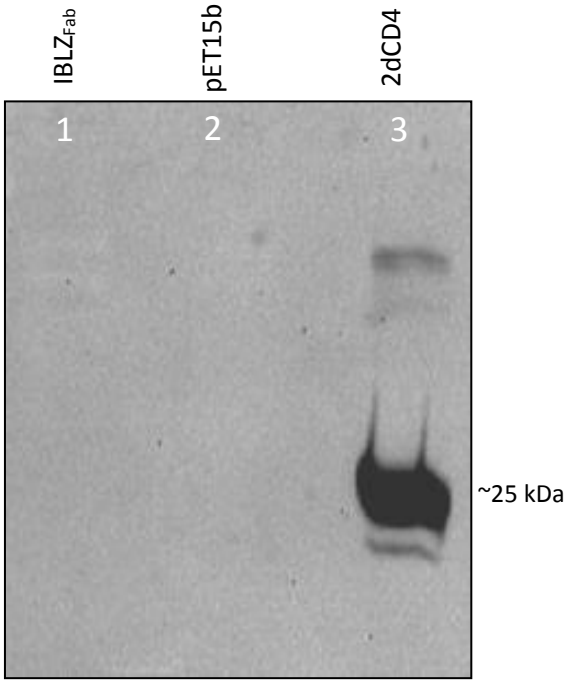

Western blot detection of histidine tagged $IBLZ_{Fab}$ and 2dCD4.

Despite the presence of a his-tag at the N terminal domain of the Fab fragment, detection with an anti his-probe was unsuccessful. A 2dCD4 his-tagged protein was run in conjunction with $IBLZ_{Fab}$ to confirm the functionality of the probe. The image shows detection of the 2dCD4 but not the Fab fragment.

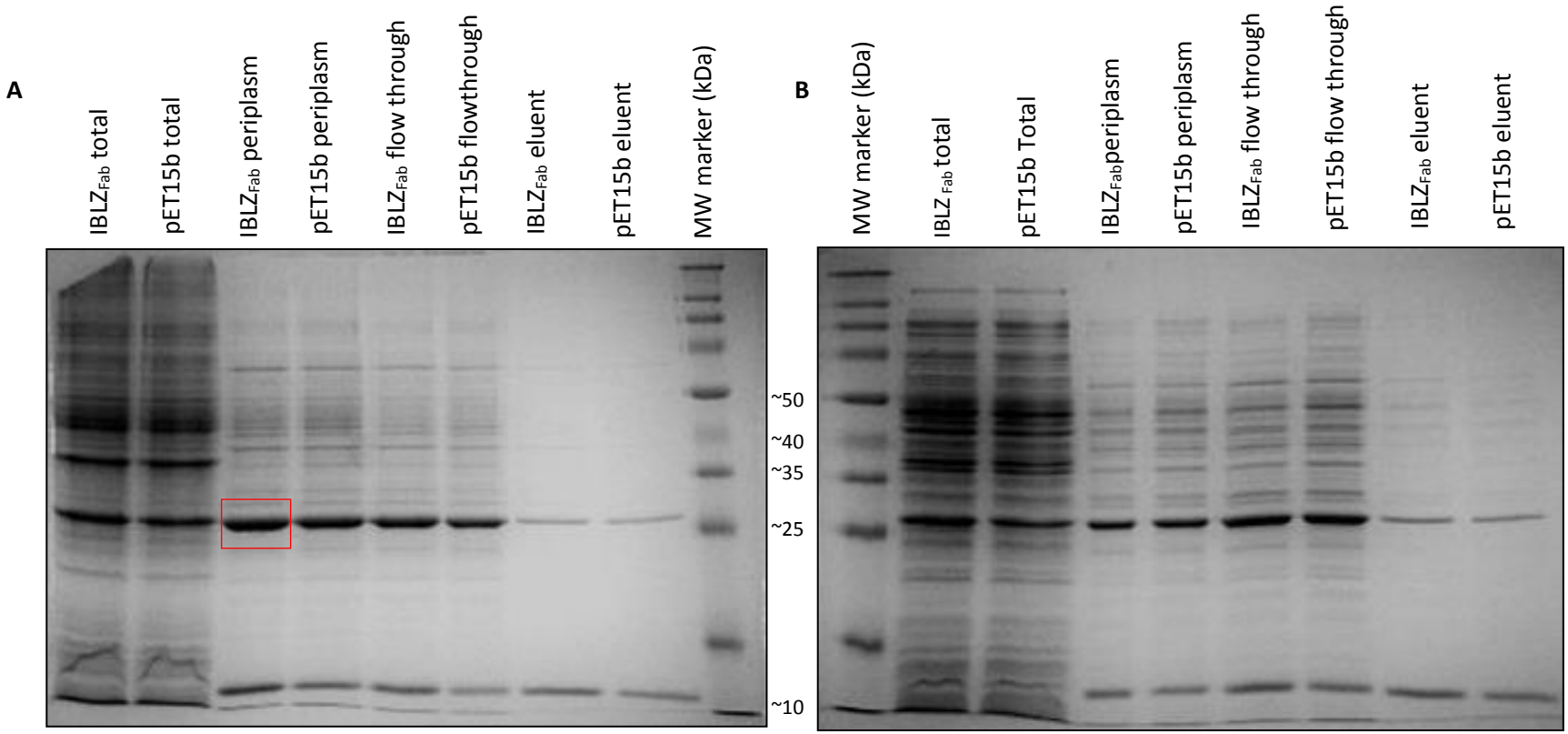

SDS-PAGE analysis of IBLZ$_{Fab}$ expression and purification:

IBLZ$_{Fab}$ was expressed in BL21 Star™ (DE3) *E. coli* cells and protein over expression was induced by cooling the incubation temperature to 30˚C for overnight expression. Samples were resolved on a 12.5 % SDS-PAGE gel and stained with Coomassie R-250 stain overnight. **(A) SDS-PAGE analysis under reducing conditions.** Reduction of samples leads to the formation of individual chains visible at ~25 kDa. The band around 25 kDa is slightly more pronounced in the periplasmic fraction of IBLZ$_{Fab}$ than the periplasmic fraction of *E. coli* transformed with empty vector. **(B) SDS-PAGE analysis under non-reducing conditions.** The absence of reducing agent keeps the disulfide bond in the Fab fragment intact. The assembled IBLZ$_{Fab}$ is therefore expected to be approximately 50 kDa and the unassembled chains should be visible at ~25 kDa. Due to low expression, the Fab fragment is not distinguishable on a coomassie gel stain. It can be seen from the gels that there is no difference between the banding patterns of IBLZ$_{Fab}$-pET15b and *E. coli* transformed with empty pET15b vector. The similarities between the banding patterns could also be due to the expression of proteins in the plasmid vector that may occur as the same size to the protein of interest.

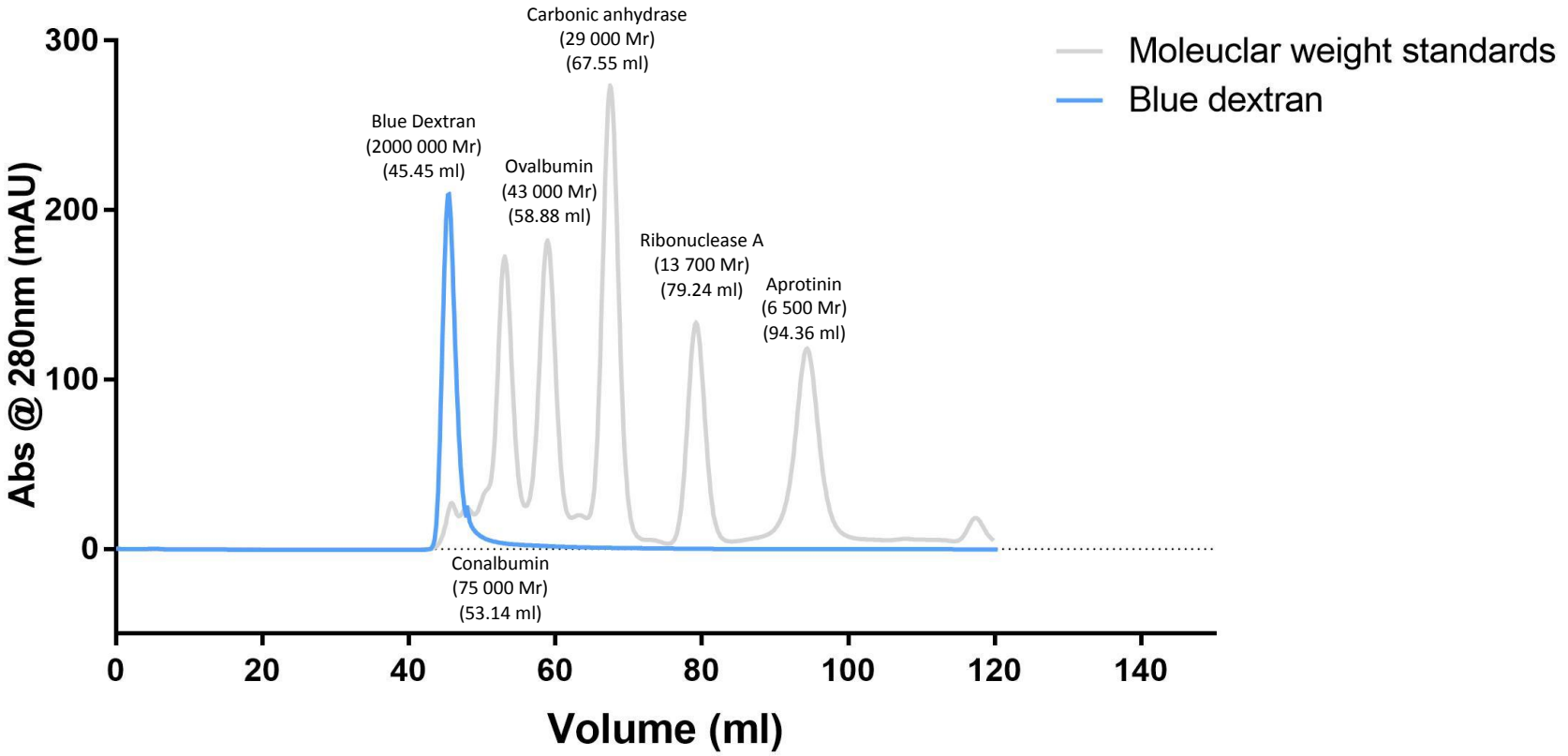

Gel filtration LMW Calibration Standards separated on a Sephadex G-75 column

In order to determine the elution volume and size of the Ibalizumab Fab fragments and fractions of interest, a gel filtration LMW calibration kit was separated on the column used. The elution of the Fab fragment occurred between the Conalbumin and Ovalbumin proteins, predicting a size of ~50 kDa. The unassembled chains which are approximately 25 kDa eluted within the Carbonic anhydrous range.